CORTEX 105 (2018) 4–25

Available online at www.sciencedirect.com

ScienceDirect

Journal homepage: www.elsevier.com/locate/cortex

Special issue: Research report

The neural correlates of visual imagery: A co-ordinate-based meta-analysis

Crawford I.P. Winlove [a,*], Fraser Milton [b], Jake Ranson [c], Jon Fulford [a], Matthew MacKisack [a], Fiona Macpherson [d] and Adam Zeman [a]

[a] Medical School, University of Exeter, UK
[b] School of Psychology, University of Exeter, UK
[c] St George's Medical School, London, UK
[d] Department of Philosophy, University of Glasgow, UK

ARTICLE INFO

Article history:
Received 4 August 2017
Reviewed 2 October 2017
Revised 11 December 2017
Accepted 18 December 2017
Published online 2 January 2018

Keywords:
fMRI
Neuroimaging
Imagery
Imagination
ALE

ABSTRACT

Visual imagery is a form of sensory imagination, involving subjective experiences typically described as similar to perception, but which occur in the absence of corresponding external stimuli. We used the Activation Likelihood Estimation algorithm (ALE) to identify regions consistently activated by visual imagery across 40 neuroimaging studies, the first such meta-analysis. We also employed a recently developed multi-modal parcellation of the human brain to attribute stereotactic co-ordinates to one of 180 anatomical regions, the first time this approach has been combined with the ALE algorithm. We identified a total 634 foci, based on measurements from 464 participants. Our overall comparison identified activation in the superior parietal lobule, particularly in the left hemisphere, consistent with the proposed 'top-down' role for this brain region in imagery. Inferior premotor areas and the inferior frontal sulcus were reliably activated, a finding consistent with the prominent semantic demands made by many visual imagery tasks. We observed bilateral activation in several areas associated with the integration of eye movements and visual information, including the supplementary and cingulate eye fields (SCEFs) and the frontal eye fields (FEFs), suggesting that enactive processes are important in visual imagery. V1 was typically activated during visual imagery, even when participants have their eyes closed, consistent with influential depictive theories of visual imagery. Temporal lobe activation was restricted to area PH and regions of the fusiform gyrus, adjacent to the fusiform face complex (FFC). These results provide a secure foundation for future work to characterise in greater detail the functional contributions of specific areas to visual imagery.

* *Corresponding author*. Medical School, University of Exeter, UK.
E-mail address: c.i.p.winlove@exeter.ac.uk (C.I.P. Winlove).

https://doi.org/10.1016/j.cortex.2017.12.014
0010-9452/

1. Introduction

Imagination has attracted human interest for at least two thousand years (Hume, 1784; Mithen, 1998; Modrak, 1987; see MacKisack et al., 2016 for a recent review), was disavowed by much of the academic community in the first half of the 20th century (Watson, 1913), then played a central role in the subsequent Cognitive Revolution (Neisser, 1967). The protean nature of imagination confounds its clear definition (Thomas, 2003), yet facilitates its implication in diverse phenomena: motivation (McMahon, 1973), memory (Yates, 2014), emotional disorders (Holmes & Mathews, 2010), prospective thought (Addis, Wong, & Schacter, 2007), breast enlargement (Willard, 1977).

We explore one specific aspect of imagination – visual imagery. This is a form of sensory imagination characterised by subjective experiences similar to perception, or at least by the mental representations that underlie such experiences (Block, 1983; Dennet, 1978), with these experiences occurring in the absence of corresponding external stimuli (Finke, 1989; Richardson, 1998). First considered by philosophers, visual imagery was influentially suggested to provide a foundation for thought (Hume, 1784), with the intentionality of images suggested to provide a secure foundation for the meaning of language (Russell, 1921). Subsequent work powerfully challenged this view (Wittgenstein, 1953), and was followed by compelling arguments that invert the previously suggested relationship between language and imagery: much of the indeterminacy of images may actually be resolved through the addition of a language-based description (Fodor, 1975; Tye, 1991). Within cognitive science, most conceptual discussions have centred on whether the mental representations that mediate visual imagery are depictive, in that they arise from activity in a visual buffer with crucial spatial properties (Kosslyn, 1981, 2005), or propositional: one product amongst many of a syntactically structured system (Pylyshyn, 2003). These influential alternatives have been comprehensively evaluated (Thomas, 2014a; Tye, 1991); more recent enactive theories, which prioritise the role of attentional mechanisms and seem especially well-placed to explain phenomena such as perceptual and representational neglect (Bartolomeo, Bourgeois, Bourlon, & Migliaccio, 2013; Thomas, 2003), have so-far received considerably less consideration (Thomas, 2014b). Empirically, the neural events associated with visual imagery can be studied using neuroimaging. In a typical task, participants are asked to imagine a generic example of a common concrete object, such as a household item or a species of animal (D'Esposito et al., 1997; Ishai, Ungerleider, & Haxby, 2000; see Table 1 for further details). Neural events within these periods are contrasted with the patterns of activity observed at baseline, such as those observed when participants judge whether a given number is even (Mazard, Laou, Joliot, & Mellet, 2005).

Crucially, the results of these studies bear directly upon the conceptual debates. For example, an absence of activity in V1 – the putative location of a prominently visual representation – would directly challenge the depictive theory of visual imagery (Kosslyn, 1981). However, the prospect of clarification through neuroimaging, both in relation to visual imagery and more generally, has been only partly fulfilled (Aue, Lavelle, & Cacioppo, 2009). An important reason for this is the diversity of terminology used to describe human neuroanatomy, with multiple distinct terms used to refer to the same anatomical or functional brain region, or the same term used to refer to different regions (Bohland, Bokil, Allen, & Mitra, 2009). This threatens to confound meaningful discussion: how could we judge the role of fusiform face area in visual imagery without consensus as to which locations should carry this name?

The challenge of neuroanatomical nomenclature is not new (Wilder, 1896), but remained unresolved by attempts to compile comprehensive lists of names for neuroanatomical regions (Federative Committee on Anatomical Terminology, 1998), thesauri to relate these terms (Anthoney, 1993), or machine-readable ontologies (Bowden & Dubach, 2003; Rosse & Mejino, 2003; Rubin et al., 2006). Terminological problems are especially pronounced in human brain imaging, as anatomical regions in these images must be identified without immediate recourse to classical cytoarchitectural boundaries such as those of Brodmann areas. An element of standardisation was introduced through the widespread adoption of the Talairach atlas (Talairach & Tournoux, 1988), especially once these labels could be automatically applied to the coordinates of observed activation (Lancaster et al., 2000). However, such an approach is problematic (Bohland et al., 2009; Devlin & Poldrack, 2007; Evans, Janke, Collins, & Baillet, 2012; Toga & Thompson, 2007), most obviously because the atlas is based on the left hemisphere of a single brain, that of a 60-year old Caucasian woman, and therefore accurately represents neither the wider population nor any other individual.

To address this, we used the cortical parcellation of 180 areas recently released as part of the Human Connectome Project (HCP) (Glasser et al., 2016). These areas, of which 97 are newly identified, were defined on the basis of differences in cortical architecture, function, connectivity, and topography in a precisely aligned group average of 210 healthy young adults. This new resource is highly regarded (Gilmore, Diaz, Wyble, & Yarkoni, 2017; Jenkinson, Bannister, Brady, & Smith, 2002; Okano & Yamamori, 2016), and used in notable recent publications (e.g., Mackey, Winawer, & Curtis, 2017; Moreira, Marques, & Magalhães, 2016; Waskom & Wagner, 2017).

The detailed interpretation of neuroimaging results is further complicated by the diversity of behavioural tasks used to evoke visual imagery but, even when studies use uncontroversial anatomical terms as well as similar methods and participants, striking differences in results remain. Perhaps the most important example of such disagreement concerns whether the activity of the primary visual cortex, V1, increases during visual imagery At least seven Functional Magnetic Resonance Imaging (fMRI) studies report that V1 is active during visual imagery (Amedi, Malach, & Pascual-Leone, 2005; Ganis, Thompson, & Kosslyn, 2004; Handy et al., 2004; Ishai et al., 2000; Klein, Paradis, Poline, Kosslyn, & Le Bihan, 2000; Lambert, Sampaio, Scheiber, & Mauss, 2002; Le Bihan et al., 1993), but at least six report that V1 is not active (D'Esposito et al., 1997; Formisano et al., 2002; Ishai et al., 2000; Knauff, Kassubek, Mulack, & Greenlee, 2000; Sack et al., 2002; Trojano et al., 2000). Such contrasting findings are striking in themselves, but have garnered particular attention because

Table 1 – Studies that examined visual imagery and were included in our ALE calculations. Also included are brief descriptions of the baseline condition and the visual imagery task from which we used co-ordinates.

Author	Year	Baseline task	Visual imagery task	Sub-groups
Kosslyn	1993	View lower-case letter	Same letter in upper-case, superimposed on grid; judge superposition of probe	
Roland	1995	Recognition of trained pattern	Imagine series of trained patterns	A, C
Kosslyn	1995	Aural common object and spatial comparison	Imagine large -size image: trained concrete object	A, B, C
Mellet	1996	Aural words phonetically similar to instructions	Imagine completed assembly of 12 connected 3D cubes, following instructions	A, B, C
Kosslyn	1997	View canonical and non-canonical images of objects; view letters	Upper-case letter superimposed on grid, after viewing lower-case letter; judge superposition	
D'Esposito	1997	Aural abstract words	Imagine common concrete object	A, B, C
Mellet	1998	"Rest"	Imagine common concrete object	A, B
Ishai	2000	View grey square	Imagine familiar concrete object: directed to house/chair/face	
Knauff	2000	View pattern superimposed on grid	Imagine familiar pattern superimposed on grid; judge superposition	
Mellet	2000	T/F to "comparison statements"	Imagine trained set of geometric objects; judge relative height of components	A, B, C
Trojano	2000	View analogue clock; spatial judgement of angle between clock hands	Imagine aural time; spatial judgement of angle between clock hands	A, B, C
Gulyás	2001	Defocused thought	Imagine capital letters (alphabet or first letter of successive words in national anthem)	A, B
Thompson	2001	Button press for 3rd neutral word in series	Imagine two trained patterns; judge relative dimensions	A, C
Formisano	2002	Fixate cross	Imagine written time; spatial judgement of angle between clock hands	
Ishai	2002	View letter string	Imagine celebrity (grouped Short-Term Mem – earlier in session – & LTM – No prior viewing)	
Sack	2002	Rest: the brief period between trials	Imagine aurally presented time; spatial judgement of angle between clock hands	
Lambert	2002	Aural abstract words	Imagine common concrete object: animals	A, B, C
Vanlierde	2003	Aural abstract words	Imagine pattern superimposed on grid; judge symmetry	A, C
Mechelli	2004	View grey square	Imagine familiar concrete object: choice of house/chair/face	
Yomogida	2004	Fixate cross	Imagine familiar concrete object	B
Ganis	2004	Rest: the brief period between trials	Imagine trained line-drawing of concrete object; answer property-related question	A,
Belardinelli	2004	View neutral sentence describing abstract concept	Imagine familiar concrete object	B, C
Handy	2004	Aural abstract words	Imagine common concrete object	A, B, C
Amedi	2005	"Rest"	Imagine familiar concrete object	A, B
Mazard	2005	T/F to letter as vowel and evenness of number	Imagine trained line drawing	A, B, C
Gardini	2005	Read visual pseudo-word; button press on its appearance	Imagine general example of common concrete object	B, C
Kosslyn	2005	Respond to visual cue with button press	Imagine visually trained pattern; judge whether probe would overlap with imagined pattern	C
Kukolja	2006	View analogue clock; spatial judgement of angle between clock hands	Imagine written time; spatial judgement of angle between clock hands	C
Kukolja	2006	Aural abstract words	Imagine written time; spatial judgement of angle between clock hands	
Belardinelli	2009	Aural abstract words	Imagine common concrete object	B, C
Gardini	2009	Aural pseudo-words	Imagine general example of common concrete object	B, C
Palmiero	2009	Aural pseudo-words	Imagine general example of common concrete object	B, C
Zeman	2010	View letter string	Imagine famous face	
Lacey	2010	Aural word-pair judgment	Imagine two common concrete objects; judge similarity of shape	A, C
Huijbers	2011	Unsuccessful imagery	Successful imagery: grouped visual imagery and auditory imagery of common concrete objects	C
de Borst	2012	Fixate cross	Imagine trained scene: room with three objects; judge whether probe is a component	
de Araujo	2012	View scrambled image	Imagine trained concrete object: people, animal or tree	
Zvyagintsev	2013	Count-back	Imagine familiar concrete object	B, C
Bien	2014	Fixate cross	Imagine aurally presented time; spatial judgement of angle between clock hands	
Boccia	2015	Fixate cross	Visuo-spatial imagination: grouped clock, navigational and geographical tasks	
Bonino	2015	Two aural times – judge chronological order	Imagine aural time; spatial judgement of angle between clock hands	C

Note: The sub-groups column identifies those studies which were also used in sub-group comparisons, with group A comprising those in which participants had their eyes closed, group B imagery generation tasks, and group C activation relative to an active baseline.

Table 2 – Areas consistently activated in the overall comparison of visual imagery studies.

Cluster number	Volume (mm^3)	Focus co-ordinates (MNI)			Reference	Anatomical label	
		X	Y	Z		Talairach daemon	Multi-modal parcellation, Glasser et al., 2016
1	8952	−26	−68	48	a	Sup. parietal lobule, BA7	Medial intraparietal area
		−41	−47	51	b	Inferior parietal lobule, BA40	Area PFm complex
		−30	−77	35	c	Sup. occipital gyrus	Intraparietal area 0
2	3760	−47	5	30	d	Precentral gyrus	Rostral area 6
		−43	26	28	e	Middle frontal gyrus	Area posterior 9-46v
3	3280	−5	12	49	f	Sup. frontal gyrus	Supplementary and cingulate eye field
		10	21	46	g	Medial frontal gyrus	Area 8BM
		−5	5	38	h	Cingulate gyrus, BA24	Posterior 24 prime
4	2192	−3	−77	4	i	Lingual gyrus	V1
		8	−83	11	j	Cuneus	V1
		−3	−88	−4	k	Lingual gyrus, BA18	V1
5	1584	52	−56	−13	l	Fusiform gyrus, BA37	Area PH
6	1512	25	−70	45	m	Precuneus, BA7	Intraparietal sulcus 1
		18	−62	29	n	Precuneus, BA31	Parieto-occipital sulcus area 2
7	1424	37	24	−5	o	Insula, BA13	Anterior ventral insular area
		45	20	−1	p	Insula	Area 44
8	1280	−31	20	−2	q	Insula	Anterior ventral insular area
		−33	22	6	r	Insula, BA13	Frontal opercular area 4
9	1232	−30	−4	55	s	Precentral gyrus, BA6	Area 6 anterior
10	1136	−47	−57	−13	t	Fusiform gyrus, BA37	Area PH
11	1088	33	−4	52	u	Precentral gyrus, BA6	Area 6 anterior
		31	9	60	v	Middle frontal gyrus	Inferior 6–8 transitional area

Note: The total volume of each cluster is reported, as well as the individual foci within it which reached statistical significance. For convenience, each individual focus is also referenced by a single letter in Fig. 2 and the main text. Individual foci are identified using anatomical labels from the parcellation of Glasser et al. (2016). To facilitate comparison with the existing literature the labels provided by the Talairach daemon (Lancaster et al., 2000) are also provided, including Brodmann cytological areas if these were also indicated. Some foci do not have a Brodmann area, because no such label was nearby. The differences between the Glasser and Talairach terms illustrates the greater anatomical accuracy made possible through the recent multi-modal parcellation. The minimum cluster size for this comparison was 1032 mm^3.

they bear on the vigorous debate, mentioned above, as to whether the mental representations mediating visual imagery are depictive (Kosslyn, 1981, 2005), or propositional (Pylyshyn, 2003). Other points of discussion have included whether activation during imagery is bilateral or strongly lateralised (cf. Gardini, Cornoldi, De Beni, & Venneri, 2009; Zvyagintsev et al., 2013; see Kosslyn, Thompson, Sukel, & Alpert, 2005 for review), and whether anatomically similar regions in each hemisphere mediate different aspects of imagery: for example, image generation in the left parietal lobe and spatial comparisons in the right (Boccia et al., 2015; Mazard et al., 2005).

Why do so many points of disagreement remain? One reason is that the small sample sizes typical of neuroimaging studies have low statistical power; studies whose results do reach significance are then difficult to replicate because, despite their large effect sizes, these are unrepresentative (Button et al., 2013; David et al., 2013). Further complications arise from the variety of analytical approaches used in neuroimaging (Carp, 2012; Glatard et al., 2015). Within the literature on visual imagery, these issues are compounded by the fact that many studies took place early in the development of neuroimaging techniques, using statistical thresholds which would now be considered inappropriately lenient. Finally, separate to the challenges of anatomical labelling that arise from the sheer complexity of the human brain (Mai & Paxinos, 2012) there remains the seductive allure of ascribing activation to particular anatomical regions on the basis of these regions' popularity or theoretical convenience (Behrens, Fox, Laird, & Smith, 2013).

The impact of these issues can be minimised through co-ordinate based meta-analysis, a family of approaches for analysing neuroimaging data which maximise power and objectivity whilst removing the effects of inconsistencies in anatomical labelling. We used the most popular algorithm for coordinate-based meta-analysis, Activation Likelihood Estimation (ALE, Eickhoff et al., 2016), the key feature of which is that reported foci are not treated as definite locations, but rather as the central point in a three-dimensional Gaussian distribution (Eickhoff et al., 2009). The foci from a single study are represented in a modelled activation map, thereby preserving the characteristic spatial relationship between foci, then voxel-wise ALE scores are calculated through the combination of the individual maps. Finally, the true convergence of foci is distinguished from random clustering by testing against the null-hypothesis of a random spatial association between experiments (Eickhoff, Bzdok, Laird, Kurth, & Fox, 2012; Turkeltaub, Eden, Jones, & Zeffiro, 2002). Over 700 papers using the ALE algorithm have been published in the last decade. The work reported here, based on data from 464 participants and 40 papers, is the first to apply the method to the study of visual imagery. To the best of our knowledge, our study is also the first to combine the 180-region multi-modal parcellation of Glasser et al. (2016) with co-ordinate based meta-analysis using the ALE algorithm.

2. Methods

2.1. Data collection

We used five portals to search for articles: the Web of Knowledge suite (WoK), PubMed, Embase, PsycINFO, and CINAHL. To ensure our searches were comprehensive and objective we optimised our search terms using text analytics. We therefore performed an initial search of the MEDLINE database via the WoK for papers with visual imagery in their title, and compiled the abstracts of the 50 most-cited papers in a single text document. We then used a Corpus Type Frequencies Grid to rank the words within this document by frequency (Taporware, Hermeneuti project). We excluded from this analysis the standard Taporware list of English Stop Words. This approach allowed us to supplement our original search terms with additional key words, whilst avoiding introducing our own bias; the full search-terms and algorithms are provided in the supplementary material.

Our final searches identified a total of 4069 papers on the 15th June 2016. Papers were removed from this sample if they did not study humans (224), were not written in English (350), or were not one of the following: an article, meta-analysis, case report, letter, abstract or clinical trial (270). Of the remaining articles, 1118 were duplicates and were therefore removed. Four members of the research group read the abstracts of the remaining 2107 papers to establish their suitably on the basis of our *a priori* criteria.

Inclusion criteria were that: 1) participants were healthy; 2) the papers were fMRI or PET experiments; 3) the papers investigated the imagery of scenes or objects, including faces, that did not require the involvement of any modality other than vision; 4) activation foci were given as 3D stereotactic (*x*, *y*, *z*) coordinates reported in Talairach or Montreal Neurological Institute (MNI) format. PET studies were included as a previous ALE meta-analysis of motor imagery had successfully incorporated both methodologies (Hetu et al., 2013), as have highly-influential ALE studies in other psychological domains (e.g., Binder, Desai, Graves, & Conant, 2009). Exclusion criteria were that: 1) the study data were already included through another identified publication; 2) the imagery task would draw prominently on more than one sensory modality.

The application of the inclusion and exclusion criteria in screening the abstracts yielded a short-list of 75 papers. 49 of these papers were subsequently excluded for the following hierarchy of reasons: we were unable to find a copy of the paper (10), they were reviews (4), they did not actually report co-ordinates and requests for this information from the authors were unsuccessful (23), they did not actually examine visual imagination (11), they reported areas shared by imagery and a cognitive process purposefully activated in a separate task (1). We searched the bibliographies of the remaining 26 papers selected for inclusion, and thereby identified a further 18 papers for detailed screening; of these, 2 did not report co-ordinates, 1 was a review, and 1 had no suitable comparison task; we included the remaining 14 papers. We ultimately identified 40 papers suitable for inclusion in our meta-analysis, which are summarised in Table 1. A full list of all the papers we short-listed and the reasons for their exclusion is available as supplementary material.

2.2. Data extraction

We used activation foci identified through statistical comparisons made across the whole-brain and those restricted to regions of interest (ROI). We only included activation foci with *p*-values of <.05, but accepted values regardless of whether they were uncorrected calculations, were based on a family-wise error rate, or used a false discovery rate. Some of these studies used statistical methods which would now be considered inappropriately lenient, but we included them nonetheless as false negatives (Type-II errors) are more problematic for ALE meta-analyses than false positives (Eickhoff et al., 2012; Type-I errors, Laird et al., 2005).

ALE meta-analysis requires that study coordinates are in the same stereotactic space. We performed all calculations in Talairach space, for which the grey-matter mask used in GingerALE was developed (Eickhoff et al., 2009), and subsequently converted the final results to MNI space. Coordinates reported in MNI were transformed to Talairach space using the icbm2tal algorithm (Laird et al., 2010; Lancaster et al., 2007), which has greater accuracy than the mni2tal transformation (Brett, Johnsrude, & Owen, 2002). Where possible, coordinates that had been previously transformed to Talairach using mni2tal were transformed back to MNI using this algorithm, and then reprocessed with the icbm2tal algorithm. This introduces the hazard of compounding rounding errors, but such effects are smaller than the errors associated with the mni2tal transformation; indeed, there is evidence that the mni2tal transformation results in a poorer fit than if no conversion is applied (Laird et al., 2010).

2.3. ALE meta-analyses

Activation likelihood estimation (ALE) is a form of co-ordinate-based meta-analysis that uses probability theory to characterise the spatial convergence of foci reported by neuroimaging studies (Turkeltaub et al., 2002). We used version 2.3.6 of the GingerALE algorithm (brainmap.org) which is based upon the algorithm of Eickhoff et al. (2009) and incorporates empirically-based full-width half maxima (FWHM), and a grey-matter mask which excludes regions of white-matter from the comparison. This version also included important refinements that prevent the summation of foci from the same study which are close to each other (Turkeltaub et al., 2012) and more effectively compute the null distribution of foci (Eickhoff et al., 2012). Our calculations used an uncorrected *p* value of .001 for individual voxels (Eickhoff et al., 2012), and cluster-level family-wise error thresholding (.05), an approach which provides the best compromise between sensitivity and specificity (Eickhoff et al., 2016). For each comparison we completed 1000 control permutations, whereby GingerALE generated a random dataset with the same number of foci, participants and studies as our dataset. Based on our choices of a Family-wise error (FWE) threshold of .05 and 1000 permutations the minimum cluster volume was determined as 1 mm^3 larger than the 50th smallest value

observed across the full set of permutations; in consequence, this actual value differed between each comparison and would show minor variations between iterations. For each comparison, we report all the clusters which met this size criterion; no cluster is the result of foci from just a single study. . Within each cluster, the first individual focus was simply the highest ALE value – itself a *p*-value summed across studies. Additional individual foci were reported within clusters for voxels whose ALE value was higher than 95% of all voxels in clusters of the same extent or greater, based on our FWE error-rate of .05 (Turkeltaub et al., 2012). These individual foci form the basis of our anatomical labelling.

2.4. *Anatomical labelling*

We report the extent of activation clusters, with our detailed interpretation based on the individual foci to maximise anatomical accuracy (Eickhoff et al., 2012, 2016). Small changes in threshold, which are intrinsic to permutation-based methods, can alter the overall shape and size of the final clusters by combining otherwise separate clusters in a given calculation. The location of individual foci is more consistent than that of the encompassing clusters (Fox, Lancaster, Laird, & Eickhoff, 2014). This precision also facilitates the articulation of the substantive exclusionary statements – cognitive process A occurs if and only if the region at co-ordinates XYZ is active – which are essential for effective deductive reasoning (Poldrack, 2006).

It could be argued that such a pursuit of precision is inappropriate given the different approaches used in the contributing studies to image registration and normalisation (Bohland et al., 2009; Evans et al., 2012), as well as co-ordinate transformation (Laird et al., 2010). However, whilst such effects are probably not truly random, they are also unlikely to show sufficient consistency between the contributing studies to survive the statistical thresholding that forms part of the meta-analysis procedure.

To optimise anatomical accuracy, given the well-established limitations of the Talairach and Tournoux (1988) atlas (Devlin & Poldrack, 2007), we used the cortical parcellation of 180 areas recently released as part of the HCP (Glasser et al., 2016). These areas, of which 97 are newly identified, were defined on the basis of differences in cortical architecture, function, connectivity, and topography in a precisely aligned group average of 210 healthy young adults. For further contextual and cytological detail the work of Mai and Paxinos was invaluable (2012). Such an approach risks isolating our work from the existing literature, so our tables also include the anatomical labels and Brodmann area for each focus as provided by the widely-used Talairach daemon (Lancaster et al., 2000).

2.5. *Image preparation*

For illustration, GingerALE images of significant convergence were transformed to MNI space using the FMRIB's Linear Image Registration Tool (FLIRT) in FMRIB Software Library (FSL) (Jenkinson et al., 2002). Volumetric images show activations on the R440 group average T1-weighted image released as part of the HCP database (https://ida.loni.usc.edu/login.jsp). The accompanying surface images used the surface mapping command in the Connectome Workbench (V1.2.3) to display volume data on the mid-thickness inflated brain based on the same 440 participants. The co-ordinates of individual foci were super-imposed on these images as points of 5 mm diameter. Final images were prepared using CorelDraw Graphics Suite 2017 (v. 19.0.0.328, Corel Corporation, Ottawa, Canada).

3. Results

We identified a total 634 foci in 40 individual experiments, based on measurements from 464 participants (64% Male, >95% right-handed, mean age 25.9 ± 4.8 years). Our first calculation combined all of these results, and thereby identified the areas most consistently activated during visual imagery. Additional comparisons based on sub-groups of studies allowed us to identify the neural correlates of imagery when participants had their eyes closed (Table 3), when the task involved only the generation of a common concrete object (Table 4), or when a comparison was made relative to a baseline other than rest (Table 5).

The overall comparison identified 11 clusters of consistent activation and 22 individual foci within these clusters; four of these clusters were in the right hemisphere (Table 2). In all our comparisons, the resulting activation was often deep within sulci, but never in sub-cortical structures. The mid-thickness cortical surface, which is halfway between the pial and white matter surfaces, makes it easier to see these activations (Fig. 1).

Specifically, we observed bilateral activation of the posterior parietal cortex (PPC), with the extensive activation of the left hemisphere occupying a substantially larger volume than the activation of the right hemisphere: 8952 mm^3 compared to 1512 mm^3. In the left hemisphere there was strongly overlapping activation in intraparietal area 1 (IP1, Choi et al., 2006), and more modest overlap in intraparietal area 2 (IP2, Choi et al., 2006). As illustrated in Fig. 2, this contiguous cluster encompassed three individual foci: superiorly, in the medial intraparietal area (a, MIP, Van Essen, Glasser, Dierker, & Harwell, 2012); posteriorly, in the recently identified intraparietal area 0 (c, IP0, Glasser et al., 2016); anteriorly, at the superior margin of the area PFm complex (b, Nieuwenhuys, Broere, & Cerliani, 2015). In the right hemisphere the medial intraparietal area was activated, as it was in the left hemisphere, with individual foci in area 1 of the intraparietal sulcus (m, IPS1, Hagler, Riecke, & Sereno, 2007) and area 2 of the parieto-occipital sulcus (n, POS2, Glasser et al., 2016).

The second largest cluster of activation, with a volume of 3760 mm^3 centred on rostral area 6 of the left premotor cortex (6r, Amunts et al., 2010), with an individual focus also in this area (d), and extended rostrally to a second focus in area posterior 9-46v of the orbital and polar frontal cortex (e, p9-46v, Petrides & Pandya, 1999). The superior premotor areas were activated bilaterally, with a cluster of 1232 mm^3 in the left hemisphere that encompassed an individual focus in the anterior part of area 6 (s, 6a, Fischl et al., 2008), and extended into the superior part of the frontal eye field (FEF, Glasser & Van Essen, 2011). Activation in the right hemisphere also contained an individual focus in the anterior part of area 6 (u),

Table 3 – Areas consistently activated in the eyes closed comparison of visual imagery studies.

Cluster number	Volume (mm^3)	Focus co-ordinates (MNI)			Reference	Anatomical label	
		X	Y	Z		Talairach daemon	Multi-modal parcellation, Glasser et al., 2016
1	7136	−28	−70	46	aa	Precuneus, BA19	Intraparietal area 1
		−32	−54	43	bb	Parietal lobe, sub-gyral	Lateral intraparietal dorsal area
		−47	−43	46	cc	Inf. parietal lobule	Intraparietal area 2
2	2296	−3	−88	−4	dd	Lingual gyrus, BA18	V1
		4	−89	5	ee	Lingual gyrus, BA18	V1
3	2040	50	−56	−13	ff	Fusiform gyrus, BA37	Area PH
4	1416	−47	−57	−13	gg	Fusiform gyrus, BA37	Area PH
5	1304	−41	7	27	hh	Inferior frontal gyrus, BA9	Area IFJp
		−45	−1	37	ii	Precentral gyrus, BA6	Premotor eye field
6	1152	29	−70	45	jj	Precuneus, BA7	IPS1
7	1144	−5	15	49	kk	Sup. frontal gyrus, BA6	Supplementary and cingulate eye fields
		8	15	49	ll	Sup. frontal gyrus, BA6	Supplementary and cingulate eye fields
		3	17	46	mm	Med. frontal gyrus	Area 8BM
8	816	−33	−2	52	nn	Precentral gyrus, BA6	Frontal eye field

Note: The total volume of each cluster is reported, as well as the individual foci within it which reached statistical significance. Individual foci are referenced by a single letter in Fig. 2 and main text. Individual foci are identified using anatomical labels from the parcellation of Glasser et al. (2016). To facilitate comparison with the existing literature the labels provided by the Talairach daemon (Lancaster et al., 2000) are also provided, including Brodmann cytological areas where also indicated. Some foci do not have a Brodmann area, because no such label was nearby. The minimum cluster size for this comparison was 712 mm^3.

with another focus in the inferior 6–8 transitional area of the dorsolateral prefrontal cortex (v, i6-8, Triarhou, 2007). This right hemisphere cluster measured 1088 mm^3 overall and, like that in the left hemisphere, encompassed the FEF.

The third largest cluster measured 3280 mm^3 and spanned the longitudinal fissure. In the left hemisphere there was an individual focus in the supplementary and cingulate eye field (f, SCEF, Amiez & Petrides, 2009), itself a recently identified sub-region of the supplementary motor area (Glasser et al., 2016). The same cluster extended ventrally across the posterior boundary of anterior 24 prime (a24pr, Vogt & Palomero-Gallagher, 2012), with an individual focus at the superior edge of posterior 24 prime (h, p24pr, Vogt & Palomero-Gallagher, 2012). Activation in the right hemisphere extended more anteriorly than that of the left hemisphere, encompassing the SCEF but extending to an individual focus in area 8BM (g, 8BM, Glasser et al., 2016).

The largest cluster of activation in the right hemisphere, measuring 1584 mm^2, was centred in area PH, a recently redefined region of the posterior temporal cortex (Glasser et al., 2016; PH, Triarhou, 2007), with an individual focus in the same area (l). An anterior region of area PH was activated in the left hemisphere, with the individual focus part of a cluster measuring 1136 mm^3 (t). The activation in both hemispheres was lateral to the fusiform face complex (FFC) (Glasser & Van Essen, 2011).

Further activation in the right hemisphere was seen in a cluster of 1424 mm^3, with an individual focus and prominent activation in the anterior ventral insular area (o, AVI, Van Essen et al., 2012) and an individual focus at the inferior

Table 4 – Areas consistently activated in the simple generation comparison of visual imagery studies, whereby participants were instructed to imagine a common concrete object.

Cluster number	Volume (mm^3)	Focus co-ordinates (MNI)			Reference	Anatomical label	
		X	Y	Z		Talairach daemon	Multi-modal parcellation, Glasser et al., 2016
1	1952	−9	11	54	aaa	Med. frontal gyrus	Supplementary and cingulate eye fields
2	1944	−47	−66	−14	bbb	Fusiform gyrus	Fusiform face complex
		−45	−59	−13	ccc	Fusiform gyrus	Area PH
		−62	−68	−10	ddd	Mid. occipital gyrus	Area PHT
3	1240	−30	−68	48	eee	Precuneus	Intraparietal area 1
		−28	−75	28	fff	Temporal lobe, sub-gyral	Intraparietal area 0
		−26	−77	40	ggg	Precuneus	Intraparietal sulcus 1
4	936	−41	9	29	hhh	Inf. frontal gyrus	IFJp
		−43	21	24	iii	Mid. frontal gyrus	IFSp
5	880	50	−56	−16	jjj	Fusiform gyrus, BA37	Area PH

Note: The total volume of each cluster is reported, as well as the individual foci within it which reached statistical significance. Individual foci are referenced by a single letter in Fig. 4 and main text. Individual foci are identified using anatomical labels from the parcellation of Glasser et al. (2016). To facilitate comparison with the existing literature the labels provided by the Talairach daemon (Lancaster et al., 2000) are also provided, including Brodmann cytological areas where also indicated. Some foci do not have a Brodmann area, because no such label was nearby. The minimum cluster size for this comparison was 840 mm^3.

Table 5 – Areas consistently activated in the active baseline comparison of visual imagery studies, whereby participants were instructed to imagine a common concrete object.

Cluster number	Volume (mm^3)	Focus co-ordinates (MNI)			Reference	Anatomical label	
		X	Y	Z		Talairach daemon	Multi-modal parcellation, Glasser et al., 2016
1	4272	−28	−70	40	x1	Precuneus, BA19	Intraparietal area 1
		−28	−60	46	x2	Superior parietal lobule	Intraparietal area 1
		−26	−72	24	x3	Temporal lobe, sub-gyral	Intraparietal area 0
		−30	−52	36	x4	Parietal lobe, sub-gyral	Area lateral intraparietal dorsal
2	1312	28	4	58	x5	Mid. frontal gyrus	Area 6 anterior
		30	−8	50	x6	Precentral gyrus, BA6	Area 6 anterior
3	1296	−28	−2	52	x7	Mid. frontal gyrus	Area 6 anterior
		−18	8	56	x8	Frontal Lobe, sub-gyral	Area 6 anterior
4	1288	16	−62	26	x9	Precuneus, BA31	Parieto-occipital sulcus area 2
		28	−68	40	x10	Precuneus	Intraparietal sulcus 1
		18	−70	32	x11	Cuneus	Dorsal Transitional Visual Area
5	1256	−30	18	2	x12	Claustrum	Frontal opercular area 4
6	1072	−50	6	30	x13	Inferior frontal gyrus, BA9	Rostral area 6
		−40	2	28	x14	Precentral gyrus, BA6	Area IFJp
7	792	34	22	0	x15	Insula, BA13	Anterior ventral insula area

Note: The total volume of each cluster is reported, as well as the individual foci within it which reached statistical significance. Individual foci are referenced by a single letter in the figures and main text. Individual foci are fully identified using anatomical labels from the parcellation of Glasser et al. (2016). To facilitate comparison with the existing literature the labels provided by the Talairach daemon (Lancaster et al., 2000) are also provided, including Brodmann cytological areas where also indicated. Some foci do not have a Brodmann area, because no such label was nearby. The minimum cluster size for this comparison was 736 mm^3.

edge of the overlying area 44 (p, 44, Amunts et al., 2010). The left anterior ventral insular area was also activated (q, 1280 mm^3), with an individual focus in the recently described frontal opercular area 4 (r, FOP4, Glasser et al., 2016), and activation extending into frontal opercular area 5 (Glasser & Van Essen, 2011). The primary visual cortex was activated bilaterally, as part of a cluster measuring 2192 mm^3, with two individual foci in the left hemisphere (i and k, V1, Abdollahi et al., 2014) and one focus in the right (j).

This whole-group comparison aimed to maximise the power of our calculations by incorporating the largest possible sample of studies. However, any such increase in power is offset by the considerable heterogeneity of this group. Further, the whole-group comparison cannot provide insight into the patterns of activation associated with specific types of visual imagery task. We therefore conducted a series of additional ALE calculations to explore the patterns of activation seen in homogenous sub-groups of studies. It is important to note that these comparisons are not independent of each other: an individual study could be part of the overall comparison and one-or-more sub-group comparison. Full details as to which paper is in which comparison are provided in Table 1.

3.1. *The eyes closed sub-group*

The first of these sub-groups included only those studies in which participants had their eyes closed. Such a comparison addresses the often-contentious issue of whether imagery activates primary visual areas (Kosslyn & Ochsner, 1994; Roland & Gulyás, 1994a) by removing the possibility that this area is stimulated directly by external cues. These calculations, which were based on 322 foci from 19 experiments and 179 participants, showed an overall pattern of activation that was similar to that seen in the whole-group comparison, in terms of localisation and lateralisation, but with smaller clusters of activation. In total, we saw eight clusters of activation and 15 individual foci (Table 3, Fig. 3). These areas included the activation of V1, whilst four of the areas active in the whole-group comparison were no-longer active: the bilateral anterior ventral insular, the neighbouring area 44, and frontal opercular area 4. In other regions overlap now arose in anatomically distinct but adjacent areas – for example, intraparietal area 0 rather than 1.

The largest cluster of activation was once again in the left PPC (7136 mm^3). Activation within this cluster encompassed area 1 of the intraparietal sulcus and the medial intraparietal area; the cluster's rostral extension included individual foci in intraparietal areas 1 and 2 (aa, IP1; CC; IP2) and in the lateral intraparietal dorsal area which adjoins intraparietal area 2 (bb, LIPd, Van Essen et al., 2012). In the contralateral hemisphere, activation in this region was restricted to area 1 of the intraparietal sulcus (jj, 1152 mm^3). The second largest cluster, measuring 2296 mm^3, was centred in the primary visual cortex and contained two individual foci, one in each hemisphere (left, dd; right, ee); in the right hemisphere activation extended slightly into V2. Area PH was activated bilaterally (left, gg, 1416 mm^3; right, ff, 2040 mm^3), with activation in the left hemisphere extending slightly into the FFC.

There were individual foci in the anterior part of the SCEF in both hemispheres (left, kk; right, ll), with activation in the right hemisphere extending anteriorly into area 8BM (mm); this cluster had a volume of 1144 mm^3. The remaining clusters of activation were in premotor regions of the left hemisphere. There were two individual foci in a cluster of 1304 mm^3, one in the recently identified area IFJp (hh, IFJp, Glasser et al., 2016) and another in the premotor eye field (ii, PEF, Amunts et al., 2010). Superiorly there was an individual focus in the left frontal eye field (nn, FEF), part of a 816 mm^3 cluster.

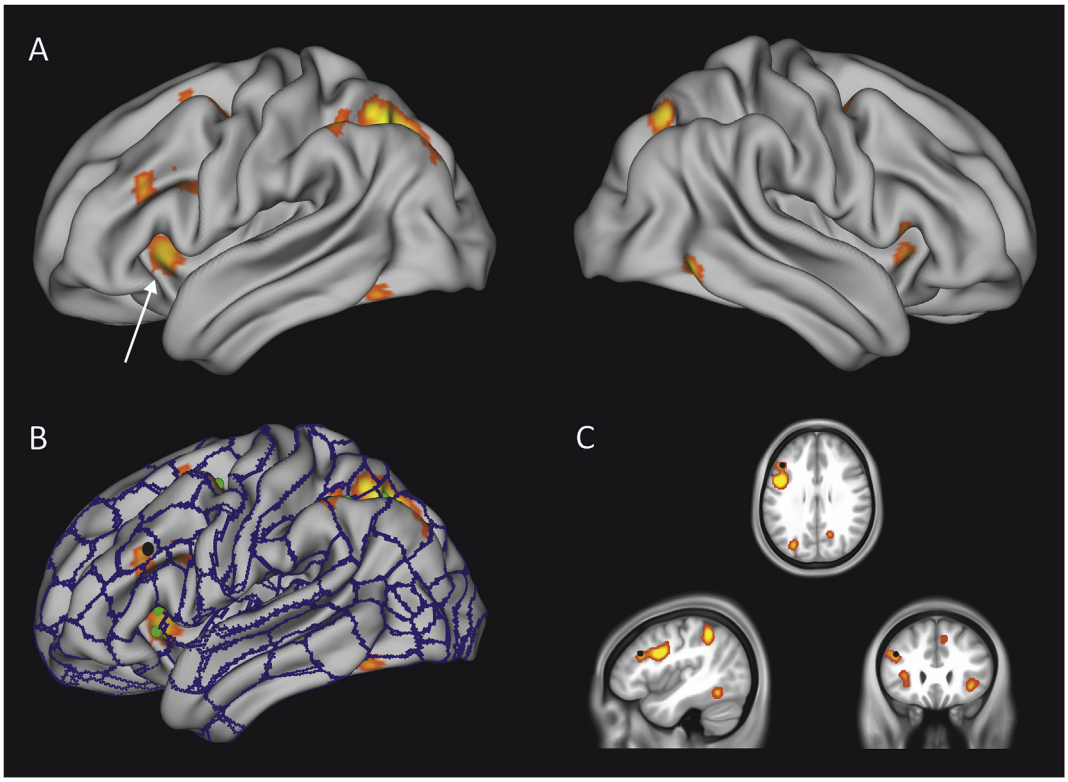

Fig. 1 – Areas consistently activated in the overall comparison of visual imagery studies. A) A lateral view of the left and right hemispheres based on the mid-thickness cortical surface, halfway between the pial and white matter surfaces, which were released as part of the Human Connectome Project (see Methods). The likelihood that a given area is consistently activated increases towards the yellow end of the red-yellow colour spectrum; absolute values are not provided as they reflect ALE scores rather than readily-interpretable probability values (Eickhoff et al., 2016). The mid-thickness semi-inflated template shows in single view areas of activation which would either not be visible simultaneously, or not visible at all – for example, the insula (marked by a white arrow) would normally be covered by the frontal, temporal and parietal opercula. This template used in all subsequent images. B) A lateral view of the left hemisphere, overlain with the 180 region-per hemisphere parcellation of Glasser et al. (2016), and individual foci reported in Table 2 projected as spheres of 5 mm diameter. Individual foci are green, with the exception of the focus in posterior 9-46v, the colour of which is changed to black to make it easier to see in part (C. The frequent proximity of foci areal boundaries, and the small size of these individual areas, is notable. C) Axial, sagittal and coronal sections volume-based images, using the 440 group average T1-weighted image (see Methods). This template is used in all subsequent images. These slices are centred on the black focus in part (B), which lies in posterior 9-46v of the orbital and polar frontal cortex (E in Table 2). The axial and coronal sections show how activation extends deep into sulci, with the coronal section also showing the extent of activation around the insula.

3.2. *The simple generation sub-group*

The second sub-group we compared characterised the activation present during the visual imagery of a common concrete object, such as an animal or a chair. This is an explicit test of imagery generation (Kosslyn et al., 2005; Mechelli, Price, Friston, & Ishai, 2004), and is less demanding than tasks which require a decision based on the attributes of the image (e.g., Formisano et al., 2002; Trojano et al., 2000). Some neuroimaging studies have examined differences in the neural correlates of imagining particular types of object – for example, faces and places – but there were too few of these studies for us to compare them. In total, we identified 16 studies and 197 foci to include in these calculations, from which we identified five clusters of activation and ten individual foci (Table 4, Fig. 4).

The largest cluster of activation (1952 mm^3), with a single individual focus (aaa), was in the left SCEF and extended laterally to areas 6a and 6ma, but not medially to the right hemisphere as it had in the eyes closed comparison. The second largest cluster of activation (1944 mm^3) spanned the central part of the FFC, with a single individual focus in this area (BBB), extending superiorly to area PH (ccc) and a further individual focus in area PHT (ddd, Triarhou, 2007). Area PH was also consistently activated in the right hemisphere (jjj, 880 mm^3). As with the other comparisons there was activation is the left PPC; there was no contralateral activation. Specifically, there were individual foci in intraparietal areas 0 and 1

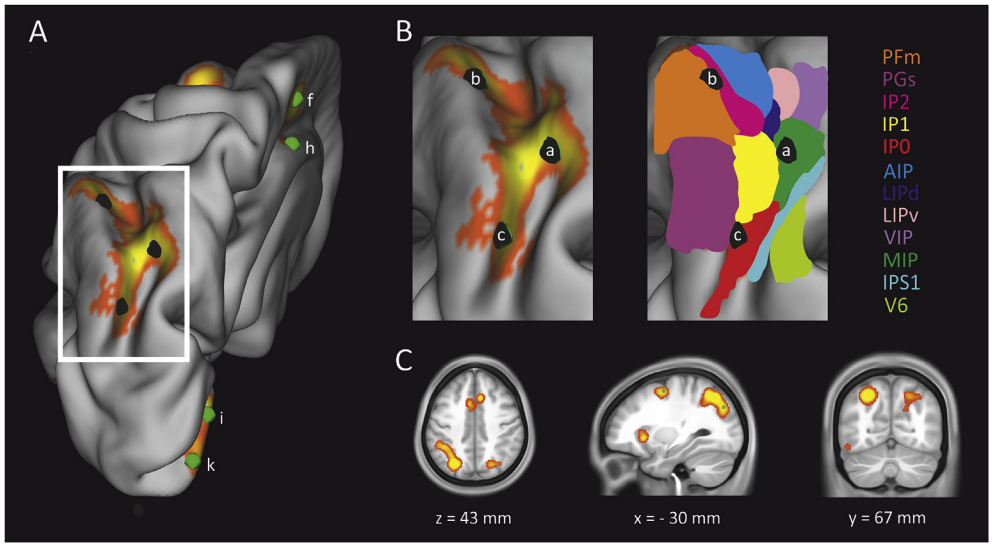

Fig. 2 – Activity in parietal areas. The left superior parietal lobe was activated in every visual imagery comparison; activation in the right hemisphere was always less extensive, and absent in the simple generation sub-group. Lower-case letters refer to foci in Table 2. A) An anterior-rostral view, from a medial aspect, of areas activated in the overall comparison. Activation extended rostrally across the superior parietal lobe, with further individual foci (green) in V1 (i, k), the supplementary and cingulate eye field (f) and posterior 24 prime (h). Premotor activation is also visible at the top of the image. The white box marks the area enlarged in section (B), the leftmost panel of which identifies the individual foci (black) in the medial intraparietal area (a), area PFm complex (b), and intraparietal area 0 (c). The panel to the right illustrates the 12 cortical areas in this region, based on the parcellation of Glasser et al. (2016), with areal colours corresponding to the colour of the accompanying text that giving their abbreviated names. Areal extents are those that are visible from the current viewing position. Most areas are defined and discussed in the main text, with the exceptions of PGs (Area PGs), AIP (anterior intraparietal area), LIPv (area lateral intraparietal ventral) and VIP (ventral intraparietal complex). C) A volume-based depiction of the same data, centred on IP1. The marked difference in the extent of consistent activation between the hemispheres is clearly visible, as is the medial activation of the supplementary and cingulate eye fields (axial section) and lateral activation of the frontal eye fields and anterior ventral insular (sagittal section) in the left hemisphere.

(fff, eee) and intraparietal sulcus 1 (ggg). Finally, we saw a cluster of activation (936 mm^3) in the inferior frontal cortex which extended anteriorly across area IFJa from an individual focus in area IFJp (hhh), to another individual focus in the recently defined area IFSp (iii, Glasser et al., 2016).

The activations of the FFC and area IFSp were novel to the simple-generation sub-group; the insula and frontal operculum were again inactive, having only been observed in the whole-group comparison. It is also notable that V1, which was active in the overall comparison and the eyes-closed group, was not active. The power of the simple-generation sub-group was sufficient for these findings to be considered robust (Eickhoff et al., 2016), so this is a notable finding.

3.3. *The active baseline sub-group*

The final sub-group comparison characterised activation during visual imagery tasks relative to an active baseline condition, such as judging whether a letter was a vowel or a number was even. This comparison enabled us to better identify components of the default mode network that are activated in visual imagery tasks but might be obscured by comparisons with a passive baseline. In total, we identified 23 experiments and 286 foci to include in these calculations, from which we identified seven clusters of activation and 15 individual foci (Table 5, Fig. 5).

The largest cluster of activation, measuring 4272 mm^2 and left lateralised, contained four individual foci; this cluster extended anteriorly from IP0 (x3) across IP1 (x1, x2) to the border of IP2 and area lateral intraparietal dorsal (LIPd, x4). Anterior area 6 was activated bilaterally, with two individual foci in both the right hemisphere (1312 mm^2; x5, x6) and the left (1296 mm^2; x7, x8). Activation in the inferior parietal lobe extended medially from an individual focus in IPS1 (x10) to foci in POS area 2 (x9) and the dorsal transitional visual area (x11), close to its boundary with V6. Further activation was seen in frontal opercular area 4 (1256 mm^2, x12), and superiorly in rostral area 6 and area IFJp (1072 mm^2; x13, x14). Finally, there was a cluster of 792 mm^2, with an individual focus in the anterior ventral insula area (x15).

4. Discussion

The aim of this study was to identify the brain regions whose activation is associated with visual imagery by performing a co-ordinate-based meta-analysis of previously published neuroimaging data. This is the first such analysis of visual

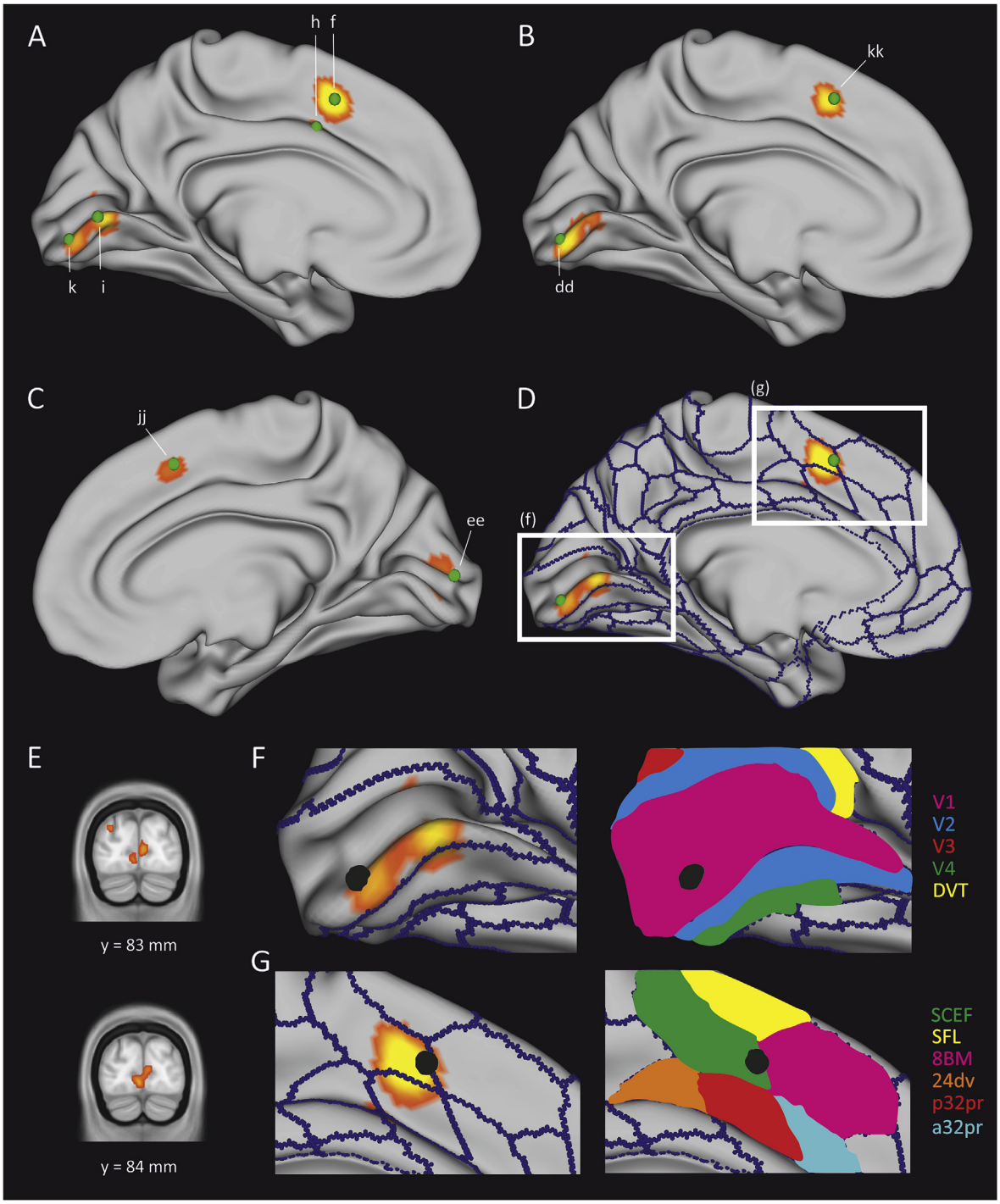

Fig. 3 – Medial areas of consistent activation in the overall comparison and in the eyes-closed sub-group comparison. Single lower case letters refer to entries in Table 2, double lower case letters to entries in Table 3. A) A lateral medial view of the left hemisphere based on the overall comparison of visual imagery studies, showing individual foci (green) in V1 (i, k), the supplementary and cingulate eye field (f) and posterior 24 prime (h). B) A lateral medial view of the left hemisphere based on the eyes closed sub-group of visual imagery studies, showing individual foci in V1 (dd) and the supplementary and cingulate eye field (kk). Compared to the overall group, activation encompasses similar areas but is less extensive. C) A lateral medial view of the right hemisphere in the eyes closed sub-group, showing individual foci in V1 (ee) and the supplementary and cingulate eye field (ll). D) The same view as shown in part (B) of the left hemisphere in the eyes closed comparison, with boundaries superimposed. The regions identified by white boxes are enlarged in panels "F" and "G". E) Axial volume-based depictions of activation in the overall comparison (top panel) and the eyes closed sub group (lower panel). F) An enlarged view of the occipital region and the five cortical areas within in it, based on the parcellation of Glasser et al. (2016), with areal colours corresponding to the colour of the accompanying text that giving their abbreviated names.

imagery data, and draws on data from 464 participants to introduce new levels of clarity and precision to this popular but often contested field. Data were entered into calculations both in combination and in a series of sub-group comparisons. In this Discussion we consider the regions activated in these comparisons lobe by lobe, before considering some important limitations to the reported work.

4.1. *Parietal lobes: the superior parietal lobule*

In our whole-group comparison we saw activation in the PPC, above the inferior parietal sulcus in the superior parietal lobule and Brodmann area 7 (Caspers, Amunts, & Zilles, 2012), with the vast majority of activation in the left hemisphere. This area has been associated with attention and working memory (Wager & Smith, 2003; Wojciulik & Kanwisher, 1999) and the top-down control of visual imagery (Mechelli et al., 2004). More specifically, we saw contiguous activation in the left hemisphere from Intraparietal Area 0 to 2, with the consistency of Intraparietal Area 1 (IP1) activation especially pronounced; IP1 was activated in every sub-group comparison. Adjacently superior and parallel to these areas we saw consistent activation in IPS1, MIP and the dorsal and ventral LIP (Fig. 1). In the right hemisphere, only IP1, IPS1 and MIP were activated, albeit at a lower level of consistency than in the left hemisphere (Fig. 1).

Previous work has linked the left PPC specifically to the generation of visual images (Bien & Sack, 2014; Knauff et al., 2000; Mechelli et al., 2004). In normal operation left-lateralised PPC activity precedes that of the right hemisphere (de Borst et al., 2012; Formisano et al., 2002). Nonetheless, activation of the left PPC is not essential for image generation: when the left PPC is temporarily lesioned using repetitive transcranial magnetic stimulation (TMS) image generation is unaffected, but can be finally disrupted with additional TMS of the right PPC (Sack, Camprodon, Pascual-Leone, & Goebel, 2005).

Variations in task demands could explain why only a relatively small part of the right posterior parietal lobe was consistently activated. The right PPC is activated during imagery tasks that necessitate explicit spatial comparisons (Boccia et al., 2015; Formisano et al., 2002; Sack et al., 2005), with the mental clock task (Paivio, 1978) the most widely-used test of spatial mental imagery. In this task, participants are presented with two times and judge which would yield the greatest angle between the hands of an analogue clock-face. Where the difficulty of this comparison is increased by small angles between the clock-hands so too is the activation of the right PPC (Bien & Sack, 2014). There were too few studies of spatial comparisons for us to compare them using ALE.

Dynamic casual modelling shows that top-down input from the superior parietal lobule to the occipito-temporal cortex is non-selective – it makes no difference whether houses, faces or chairs form the content of participants' visual imagery (Mechelli et al., 2004). These different object types are associated with distinctive patterns of activation in the occipito-temporal cortex during imagery, as they are during perception, but this arises through top-down input from prefrontal areas (ibid). The input from superior parietal regions could mediate an essential attentional component of visual imagery processes (Ishai, 2010; Ishai et al., 2000), and it is striking that the consistent activation we observed in the lateral intraparietal dorsal area (Tables 2 and 4) corresponds closely to the parietal area reliably activated during three different forms of visual attention (Wojciulik & Kanwisher, 1999). Of these, attention in the absence of stimuli may be a top-down preparatory process that supports the subsequent goal-directed selection of important stimuli and appropriate responses (Battistoni, Stein, & Peelen, 2017; Corbetta & Shulman, 2002). One might then posit a role for visual images in guiding attention itself, but to the contrary a visual search strategy based on imagery is less efficient than a strategy based on using semantic categories (Peelen & Kastner, 2011). Finally, similar superior parietal regions are activated in visual imagery and working memory (Pearson, Naselaris, Holmes, & Kosslyn, 2015), with more vivid imagery linked to better performance in visual working memory tasks (Keogh & Pearson, 2014).

4.2. *Frontal lobes*

4.2.1. *The supplementary and cingulate eye field (SCEF)*

We observed bilateral medial frontal activations centred in the SCEF. The SCEF lies on the medial surface of the superior frontal gyrus, a sub-region of the supplementary motor area (Amiez & Petrides, 2009) and Brodmann area 6 (Petrides & Pandya, 2012), most clearly distinguished from neighbouring regions by its dense myelination (Glasser et al., 2016). The SCEF adjoins the anterior cingulate and medial prefrontal cortex, which have recently been divided into 15 sub-regions (Glasser et al., 2016). The SCEF is named to reflect its functional connectivity with the frontal and premotor eye fields (areas FEF and PEF, Glasser et al., 2016). The left SCEF was active in every comparison apart from the baseline sub-group; the right SCEF was active only in the overall and eyes-closed comparisons, but differences in lateralisation should be considered cautiously given that the region adjoins the midline. Activations in this area were reported by twelve of the papers whose data were used in these calculations, and when referred to explicitly were identified as belonging to either the anterior cingulate (Yomogida et al., 2004) or the medial frontal gyrus (Ganis et al., 2004). Such terms were not inaccurate based on anatomical standards of the time, but our approach illustrates a key benefit of precise anatomical description: the

Dorsal transitional visual area (DVT) is the recently described dorsal transitional visual area. G) An enlarged view of the cingulate region and five cortical areas within it. These areas lie at the junction of four larger regions. Specifically, ventral area 24d (24dv) is part of the cingulate motor area, and SCEF part of the supplementary motor area. Area p32 prime (p32pr) is the most anterior part of the anterior cingulate and medial prefrontal cortex, of which area anterior 32 prime (a32pr) and 8BM are also components. Finally, the superior frontal language area (SFL) is part of the dorsolateral prefrontal cortex (Glasser et al., 2016). This diversity of nomenclature highlights the need for the greatest possible anatomical precision.

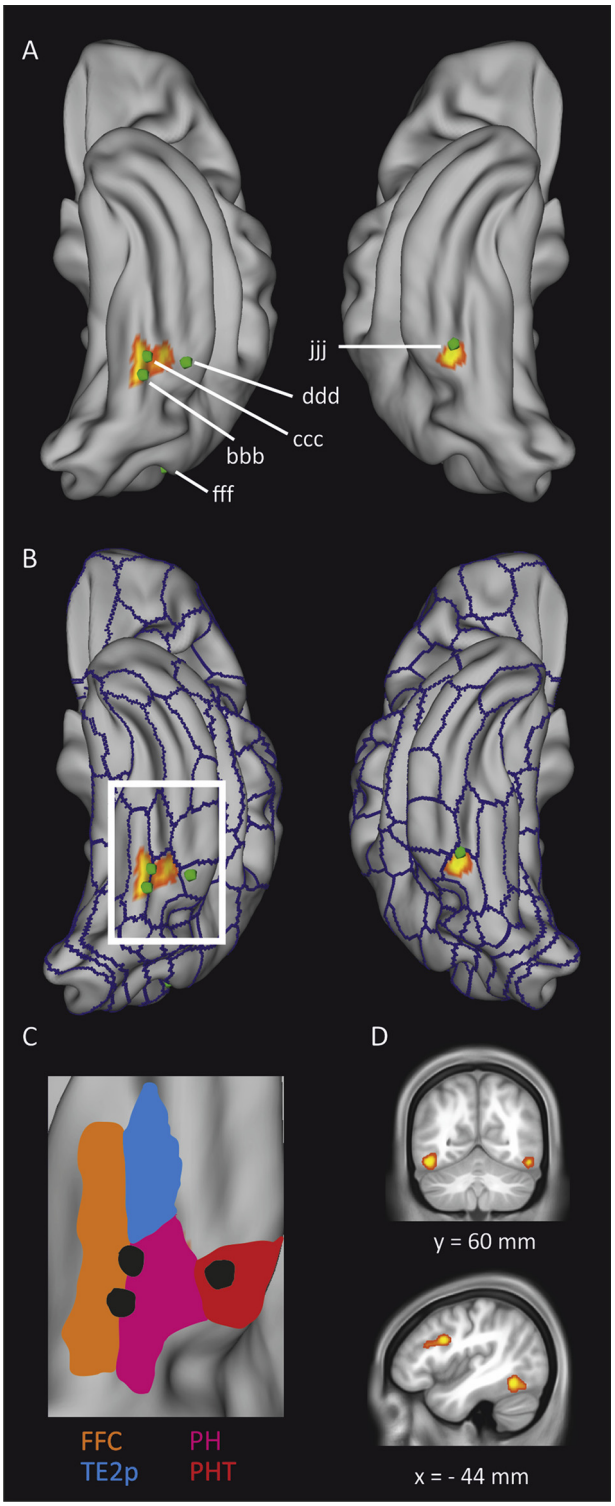

Fig. 4 – Areas of consistent activation in the simple generation sub-group comparison, which illustrate the activation of temporal areas. The labels consisting of three lower case letters refer to entries in Table 4. A) An inferior view of the left and right hemispheres, with individual foci in area PHT (PHT, ddd), area PH (PH, ccc, jjj) and the fusiform face complex area (FFC, bbb) and intraparietal area 0 (IP0, fff). B) From the same viewing angle, the cortical borders illustrated and the area expanded in "C". C) An enlarged view of the left inferior temporal lobe, showing four cortical areas; the areal colours in the right panel correspond to the colours in which the accompanying abbreviated names are written. Activation in the simple generation sub-group extends slightly into the FFC, but did not in any other comparison; for all other comparisons, the most consistent area of activation was area PH. The activation in area PHT is part of the cluster shown by the heat-map, but has been projected to the nearest cortical surface with which the activation is not contiguous. D) Axial and coronal volume-based depictions of activation baseline sub-group comparison, centred on the fusiform face complex. These illustrate how the activation might be readily, but inaccurately, interpreted as being in the fusiform face complex.

anterior cingulate label is used by at least 15% of all studies in the Neurosynth database (accessed 1st June 2017, Yarkoni, Poldrack, Nichols, Van Essen, & Wager, 2011). This presents opportunities for reverse inference on a grand scale (Poldrack, 2011), and should be viewed as highlighting the danger of anatomical imprecision rather than the region's actual involvement in diverse processes.

Early studies suggested the area we refer to as SCEF was activated during visual imagery (Gulyas, 2001; Trojano et al., 2000), and perhaps played a role in image generation as it was one of the first areas to become active during imagery (Formisano et al., 2002; Sack et al., 2002). Perhaps the most elegant evidence for the importance of the SCEF activation for visual imagery comes from the demonstration that the degree to which it is activated predicted imagery performance (de Borst et al., 2012). Specifically, SCEF activation was greater during fast than slow responses when participants correctly judged that a visually presented fragment of a scene was a mirrored component of a previously learnt complex visual scene. De Borst's dynamic model of scene imagery, informed by evidence that this region becomes active early in the process of visualisation, might suggest that activity here launches the process of visualisation through the retrieval and integration of visuospatial information. Our calculations broadly support the central role of the SCEF in visual imagery, whilst the absence of their activation in the active baseline comparison may reflect demands for working memory (Glasser et al., 2016), and the closely-allied process of attention (Gazzaley & Nobre, 2012), in the control condition in those tasks.

4.2.2. *Superior premotor areas*

We observed bilateral activation within the superior subdivision of the premotor cortex in our overall comparison: the FEF, area 6 anterior, and the inferior 6–8 transitional area (Glasser et al., 2016). The anatomical delineation of these areas has long been complicated by the high inter-individual variability of sulcal landmarks in this region (Geyer, Luppino, & Rozzi, 2012) Activation in these specific areas has received little consideration within the imagery literature, though there is evidence from dynamic causal modelling for top-down input to the temporal lobes from the wider precentral region during imagery (Mechelli et al., 2004).

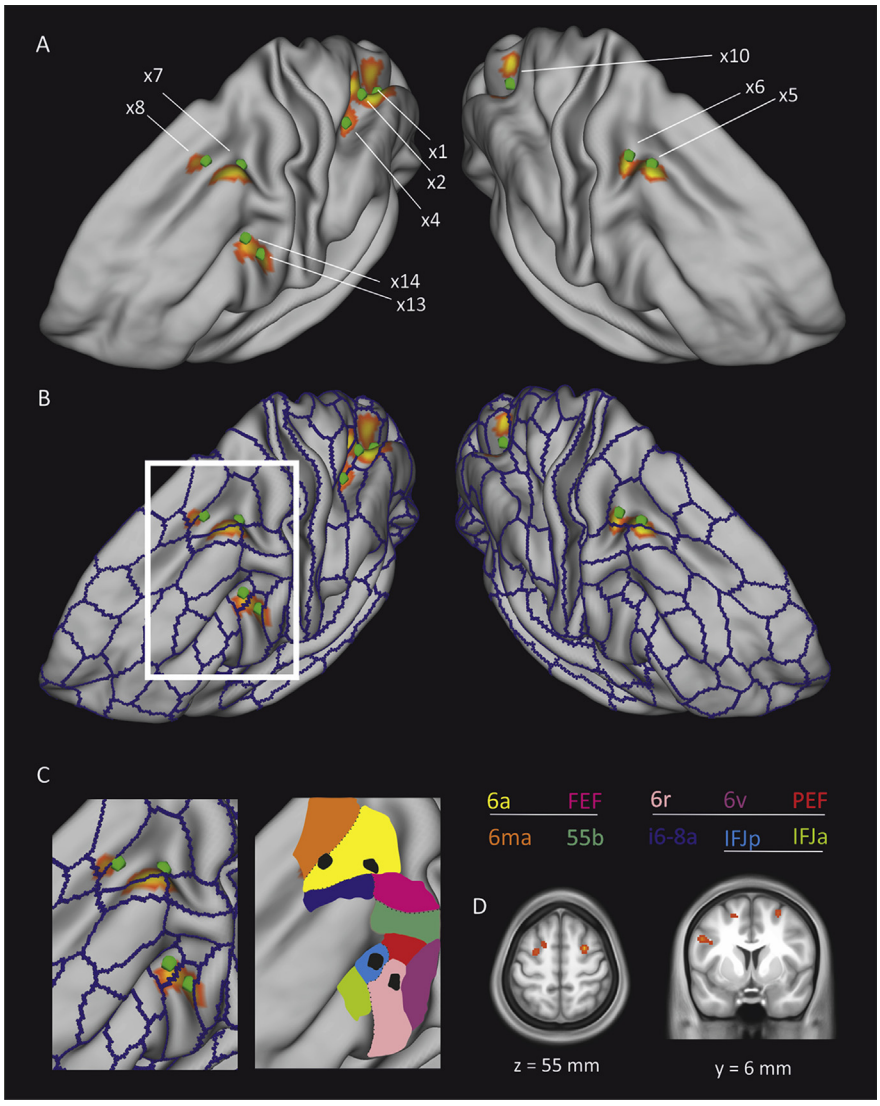

Fig. 5 – Areas of consistent activation in the active baseline sub-group comparison, which illustrate the typical activation of premotor areas. The labels consisting of a numeral and the "x" prefix refer to entries in Table 5 A) An anterior-posterior medial view of the left and right hemispheres, with individual foci in area 6 anterior (6a; x5, x6, x7, x8), area IFJp (IFJp; x14), rostral area 6 (6r, X13), area lateral intraparietal dorsal (LIPd, x4), intraparietal area 1 (IP1, x1, x2), and intraparietal sulcus 1 (IPS1, x10). B) From the same viewing angle, the cortical borders illustrated and the area expanded in "C". C) An enlarged view of centred on the inferior frontal gyrus showing nine cortical areas; the areal colours in the right panel correspond to the colours in which the accompanying abbreviated names are written, with underlining indicating areas which are part of larger anatomical regions. Specifically, 6ma is part of the supplementary motor area, 6a and FEF are parts of the superior premotor cortex, whilst 6r, 6v and PEF are part of inferior premotor cortex, from which they are divided by area 55b. Area 55b is part of the premotor cortex, but anatomically and functionally distinct from its neighbours (Glasser et al., 2016). Finally, i6-8 is part of the dorsolateral prefrontal cortex and IFJa and IFJp are part of the inferior frontal cortex. D) Axial and coronal volume-based depictions of activation baseline sub-group comparison.

It is well-established that neurons in the FEFs and neighbouring regions integrate visual and motor information to yield a retinotopic map of visual space that serves to guide the amplitude and direction of saccades (Bruce, Goldberg, Bushnell, & Stanton, 1985). It has been suggested that the continuation of such eye movements during imagery could be the basis of V1 activation (Ganis et al., 2004). Less speculatively, there is compelling evidence that the FEFs modulate visual attention through top-down input to early visual areas. For example, current injection in the macaque FEFs increases contrast sensitivity in V4 neurons during spatially-directed attention (Moore & Armstrong, 2003), and TMS of the human FEF has been associated with an increased Blood Oxygen Level Dependent (BOLD) signal in V1-4 (Ruff et al., 2006). Similar interactions were seen when activity was generated endogenously through participants performing a demanding visual

spatial attention task, work which also demonstrated that top-down input was greater than the reverse bottom-up flow of information (Bressler, Tang, Sylvester, Shulman, & Corbetta, 2008).

The scale of this top-down input makes the absence of activity in early visual areas other than V1 a surprising feature of our results. Nonetheless, this superior frontal activation may help to drive activity in posterior cortices which support the representations we experience as visual imagery.

4.2.3. *Inferior premotor areas and the inferior frontal sulcus*

We saw activation in two parts of the inferior premotor cortex, itself a part of the inferior frontal gyrus which is separated from the superior division of the premotor cortex by area 55b: rostral area 6 and the PEF (Amunts et al., 2010). These effects were strongly lateralised: neither area was active in the right hemisphere. Similar to the superior premotor cortex, these inferior regions are also of considerable anatomical complexity and functional heterogeneity (Roland & Zilles, 1996); small differences in location yield very different anatomical labels (Evans et al., 2012). For example, the focus we identify as falling in IFJp of the inferior frontal sulcus adjoins area 8C of the dlPFC, itself a rather non-specific term for an area since shown to be composed of at least 13 sub-regions (Glasser et al., 2016).

In terms of functional roles, one obvious possibility is that the activation of rostral area 6 reflects the execution of a motor task such as pressing a button to indicate whether a given probe would overlap with particular imagined pattern. Of the 16 studies that contributed to this focus, seven had no motor responses in either the baseline or imagery tasks; five used protocols that effectively controlled for motor activation through a combination of counterbalancing the response hand and baseline tasks with similar motor demands. As far as we could tell, the remaining four studies included motor responses only during the imagery tasks (Bien & Sack, 2014; de Borst et al., 2012; Formisano et al., 2002; Yomogida et al., 2004). This is a serious confound for the interpretation of these individual studies, but activation in rostral area 6 remained when these four studies were removed, suggesting activation is not due to motor demands. Activation of this area is also seen during perception (Ganis et al., 2004), with greater activation during imagery perhaps reflecting the greater difficulty of this task (Kukolja, Marshall, & Fink, 2006).

In the wider literature, activation in rostral area 6 has been clearly associated with the phonological and semantic processing of natural language (Binder et al., 2009; Poldrack et al., 1999), as have areas IFJp and IFJa of the inferior frontal sulcus and posterior 9-46v in the dorsolateral prefrontal cortex (Roland & Zilles, 1996) which are involved in semantic generation (Wager & Smith, 2003), semantic encoding (Demb et al., 1995) and semantic decision-making (Vandenberghe, Price, Wise, Josephs, & Frackowiak, 1996).

Inferior premotor areas and the inferior frontal sulcus are also highly active during tasks that require selection among competing sources of information in working memory to guide a response (Glasser et al., 2016; Thompson-Schill, D'Esposito, Aguirre, & Farah, 1997). Their activation in imagery tasks could correspond to the greater difficulty of imagery than perception – though it is striking that such activations are typically bilateral whereas the activations we observed with imagery were only in the left hemisphere.

In summary, the frontal activations, like the recruitment of the superior parietal cortex, plausibly reflect the engagement of attention and working memory, with a possible contribution from semantic processes. This meta-analysis also points specifically to the involvement of frontal lobe regions linked to the control of eye movements during visual imagery.

4.3. *Occipital lobes: primary visual cortex*

The medial part of the primary visual cortex, area V1, was activated bilaterally in our overall comparison and, more importantly, during tasks in which participants had their eyes closed. This is a notable finding, as the activation of V1 has been a point of dispute ever since the neural correlates of visual imagery were first studied. Early studies using single photon emission computerized tomography (SPECT) reported increased blood flow in the occipital cortex during visual imagery (Goldenberg et al., 1989; Roland & Friberg, 1985), but then conflicting evidence emerged (Charlot, Tzourio, Zilbovicius, Mazoyer, & Denis, 1992). A subsequent series of influential PET studies were held to show the activation of V1 during visual imagery (Kosslyn et al., 1993), with V1 activation dependent on the size of the mental image for its precise location (Kosslyn, Thompson, Kim, & Alpert, 1995) and overlapping with the activation observed during visual perception (Kosslyn, Thompson, & Alpert, 1997). However, other PET studies offered apparently contradictory evidence (Mellet, Tzourio, Denis, & Mazoyer, 1995, 1998; Mellet et al., 2000, 1996), and the interpretation of all these data was controversial (Farah, 1994; Roland & Gulyás, 1994b). A similar pattern of inconsistent findings and contested interpretations emerged as fMRI became the technique most widely used to study visual imagery. Thus, to the best of our knowledge there are at least seven fMRI studies showing V1 is active during visual imagery (e.g., Amedi et al., 2005; Klein et al., 2000; Mazard et al., 2005) and at least six showing V1 is not activated (e.g., D'Esposito et al., 1997; Ishai et al., 2000; Yomogida et al., 2004). These discrepancies could reflect the dependence of V1 activation on whether tasks require images with high resolution detail or shape judgements (Kosslyn & Thompson, 2003), as well as variations in imagery vividness (Cui, Jeter, Yang, Montague, & Eagleman, 2007; Dijkstra, Bosch, & van Gerven, 2017).

The question then still remains as to whether the activation of V1 is characteristic of visual imagery. V1 activation could simply reflect direct stimulation by visually-presented task instructions, but remained in our calculations when participants had their eyes closed. On the other hand, the simple generation comparison, in which V1 was not activated, could suggest that V1 activation is not essential for all imagery tasks. However, the simple generation calculations were based upon a small number of foci, which reduces the likelihood of convergence and thus increases the chance of a false negative. A false negative for V1 could also arise from its distinctively high level of activity at rest (Muckli & Petro, 2013), since comparisons based on univariate changes in the BOLD signal would necessitate substantial changes during a given task for its activity to reach statistical significance. It is

therefore plausible that the degree of V1 activation has previously been under-estimated.

The co-activation of areas known to provide input to V1 during visual imagery would provide circumstantial support for V1 activation. It is therefore notable that, the posterior intraparietal sulcus was extensively activated in our comparisons. There are direct connections between the posterior Intraparietal sulcus (IPS) and visual cortex in macaque (Baizer, Ungerleider, & Desimone, 1991; Lewis & Van Essen, 2000), and evidence from human fMRI that input from the posterior IPS to V1 modulates spatial attention (Lauritzen, D'Esposito, Heeger, & Silver, 2009). This modulation of spatial attention by the posterior IPS may derive from integration in the anterior IPS of input from across the frontoparietal attention network, receiving information on orientation from the superior parietal lobule (Greenberg, Esterman, Wilson, Serences, & Yantis, 2010), on distractor filtering from the inferior frontal gyri (Leber, 2010) and on eye-movements from the FEFs (Van Ettinger-Veenstra et al., 2009).

Other areas, whose co-activation with V1 might be anticipated, are conspicuous by their absence: we did not see activation of other early visual areas. We consider some possible reasons for this in the section addressing the limitations of the current work. Another possibility arises from recent studies using multivoxel pattern classification analysis (MVPA), a technique with the sensitivity to detect even small co-variations in activity across groups of voxels. These have shown activation during visual imagery across early visual areas and striking demonstrations that patterns of V1 activity are similar during the perception and imagery of simple stimuli (Albers, Kok, Toni, Dijkerman, & de Lange, 2013; Cichy, Heinzle, & Haynes, 2012; Lee, Kravitz, & Baker, 2012). However, this similarity could simply reflect consistent demands upon processes such as attention (Kamitani & Tong, 2005), reward expectation (Serences, 2008), or auditory stimulation (Vetter, Smith, & Muckli, 2014), rather than features of visual imagery *per se*. It is therefore important that voxel-wise encoding, which characterises the dependence of activation in individual voxels on separable components of retinotopic location, spatial frequency, and orientation, also found similar activation in V1 for the perception and imagery of low-level visual features (Naselaris, Olman, Stansbury, Ugurbil, & Gallant, 2015).

What is the likely functional role of V1 in visual imagery? Top-down cortical input to V1 is substantial, but lacks the inter-neuron and inter-laminar spatial precision of the bottom-up input from the lateral geniculate nucleus (Markov et al., 2014). This suggests that – even taking into account the studies using MVPA – V1 may not play the literally depictive role proposed in some theories of visual imagery, in which a close correspondence between spatial patterns of V1 activation and spatial features of represented objects is of central importance (Kosslyn, 1981, 2005). Indeed, the areas of pronounced co-activation that we observe start to suggest alternative explanations for the activation of V1 during visual imagery. For example, top-down input to V1 could serve to constrain the interpretation of otherwise ambiguous sensory information to specify imagery content, in a manner similar to that seen with the perception of a face in a white-noise visual stimulus (Smith, Gosselin, & Schyns, 2012), akin to the Pareidolia typified by falsely perceiving a common concrete objects in a cloud formations (Liu et al., 2014). More speculatively, increasing the top-down gain (Muckli & Petro, 2013) for V1 activity at rest could promote imagery experiences in the absence of any visual stimuli.

4.4. *Temporal lobes*

We observed activation in the ventral temporal cortex, where the ventral stream which mediates visual categorisation and recognition diverges across a range of functionally and anatomically discrete areas (Grill-Spector & Weiner, 2014). Bilateral activation in our overall comparison centred on the recently redefined Area PH (Glasser et al., 2016), and extended only slightly into the FFC, which lies laterally and inferiorly (Weiner et al., 2014). Five of the eight papers whose co-ordinates contributed to the cluster of activation in the left hemisphere seen in the overall comparison identified their co-ordinates as falling within the fusiform cortex, and interpreted their results in relation to this literature. For some of these studies the clusters of activation represented by these co-ordinates did indeed extend to the FFC (Belardinelli et al., 2009; de Borst et al., 2012), yet our data show Area PH to be the area in this region most consistently activated. Co-ordinates within Area PH have only rarely been reported in the wider neuroimaging literature (Yarkoni et al., 2011), though it is striking that it is strongly functionally connected to IPS1 (Glasser et al., 2016), itself one of the areas that is most consistently activated during visual imagery. One of the few neuroimaging studies to report activity in area PH showed its activity significantly decreased during the successive presentation of objects with similar physical features, independently of their semantic similarity (Chouinard, Morrissey, Köhler, & Goodale, 2008).

The question then remains, why were so few regions of the temporal lobe activated? To some extent this may reflect the residual heterogeneity between studies. It is well-established that different object types are represented at different points along the anterior-posterior axis of the temporal lobe (Ishai et al., 2000; Mechelli et al., 2004; Thompson-Schill, Aguirre, D'Esposito, & Farah, 1999). However, there were too few studies that compared specific categories of concrete object for their analysis as separate groups in the present work. It is also possible that some of the other regions active during visual imagery reduce the activity of temporal regions. For example, dynamic causal modelling shows that input from the FEF inhibits the temporo-parietal junction when informative visual stimuli are absent (Vossel, Geng, & Fink, 2014). Such stimuli are typically absent during visual imagery, whilst the FEF are consistently active. Finally, given that the hippocampus is active at rest (Stark & Squire, 2001) and is also likely to be engaged in many of the active baseline tasks (Shulman et al., 1997), its activity may remain during visual imagery but not increase sufficiently to reach statistical significance.

5. Limitations

The ALE form of co-ordinate-based meta-analysis allows the precise location of an effect across a range of tasks intended to engage a particular psychological capacity. The identified

regions are strong candidates for involvement in the process in question, but there are several important limitations to such an analysis. First, unlike meta-analyses used in other fields of research (Palmer & Sterne, 2015). ALE calculations based on neuroimaging do not consider the size of an effect; consequently, they cannot include evidence for the absence of an effect, so-called null results. Second, ALE calculations will only identify brain regions consistently activated despite differences in the associated tasks; differences between tasks may underlie the lack of activation we observed in early visual areas other than V1 and in lateral temporal regions. Third, ALE cannot illuminate the temporal dynamics of cognitive processes.

Finally, we have related our findings to the most detailed parcellation of cortical areas to-date (Glasser et al., 2016), but intrinsic features of neuroimaging modalities themselves mean the unavoidable noise in the process of brain imaging implies that localisation can only be approximate (Buxton, 2002). Ultimately, we outline a set of key regions engaged in visual imagery, whilst the execution of specific tasks is likely to engage a range of additional areas.

6. Conclusion

The work reported here is the first to combine the ALE algorithm for the co-ordinate based meta-analysis of neuroimaging data with a recently-released parcellation of the human neuroanatomy (Glasser et al., 2016), the most detailed anatomical atlas for the human yet produced. Our exploration of visual imagery, which encompassed data from 464 participants and 40 individual studies, showed imagery predominantly activated regions of the left hemisphere. The superior parietal lobule was consistently activated in all our comparisons, suggesting that attentional processes are an important aspect of visual imagery. V1 is typically activated during visual imagery, even when participants have their eyes closed, which is consistent with important depictive theories of visual imagery (Kosslyn, 1981, 2005); the absence of V1 activation in the simple generation sub-group raises a note of caution to this interpretation, whilst the lack of activation in other early visual areas is surprising. The activation of inferior premotor areas and the inferior frontal sulcus suggests that semantic operations are important for the construction and utilisation of mental images, a finding required by propositional theories of visual imagery (Pylyshyn, 2003). The activation of the superior and cingulate eye field and the FEF suggest that eye movements are also important aspects of visual imagery processes, and offer support for often over-looked enactive theories of imagery (Bartolomeo et al., 2013; Thomas, 2003).

Funding

This work was supported by funding from the Arts and Humanities Research Council for CIP Winlove, M. MacKisack, F. Macpherson and A. Zeman through a *Science in Culture Innovation Award*: *The Eye's Mind – a study of the neural basis of visual imagination and of its role in culture* (*Reference AH/M002756/1*). The research materials supporting this publication can be accessed by contacting Crawford Winlove, c.i.p.winlove@exeter.ac.uk.

Supplementary data

Supplementary data related to this article can be found at https://doi.org/10.1016/j.cortex.2017.12.014.

REFERENCES

Abdollahi, R. O., Kolster, H., Glasser, M. F., Robinson, E. C., Coalson, T. S., Dierker, D., et al. (2014). Correspondences between retinotopic areas and myelin maps in human visual cortex. *NeuroImage, 99*, 509–524. https://doi.org/10.1016/j.neuroimage.2014.06.042.

Addis, D. R., Wong, A. T., & Schacter, D. L. (2007). Remembering the past and imagining the future: Common and distinct neural substrates during event construction and elaboration. *Neuropsychologia, 45*(7), 1363–1377. https://doi.org/10.1016/j.neuropsychologia.2006.10.016.

Albers, A. M., Kok, P., Toni, I., Dijkerman, H. C., & de Lange, F. P. (2013). Shared representations for working memory and mental imagery in early visual cortex. *Current Biology, 23*(15), 1427–1431. https://doi.org/10.1016/j.cub.2013.05.065.

Amedi, A., Malach, R., & Pascual-Leone, A. (2005). Negative BOLD differentiates visual imagery and perception. *Neuron, 48*(5), 859–872. https://doi.org/10.1016/j.neuron.2005.10.032.

Amiez, C., & Petrides, M. (2009). Anatomical organization of the eye fields in the human and non-human primate frontal cortex. *Progress in Neurobiology, 89*(2), 220–230. https://doi.org/10.1016/j.pneurobio.2009.07.010.

Amunts, K., Lenzen, M., Friederici, A. D., Schleicher, A., Morosan, P., Palomero-Gallagher, N., et al. (2010). Broca's region: Novel organizational principles and multiple receptor mapping. *PLoS Biology, 8*(9), e1000489. https://doi.org/10.1371/journal.pbio.1000489.

Anthoney, T. (1993). *Neuroanatomy and the neurologic exam: A thesaurus of synonyms, similar-sounding non-synonyms, and terms of variable meaning*. Retrieved from https://www.crcpress.com/Neuroanatomy-and-the-Neurologic-Exam-A-Thesaurus-of-Synonyms-Similar-Sounding/Anthoney/p/book/9780849386312.

Aue, T., Lavelle, L. A., & Cacioppo, J. T. (2009). Great expectations: What can fMRI research tell us about psychological phenomena? *International Journal of Psychophysiology: Official Journal of the International Organization of Psychophysiology, 73*(1), 10–16. https://doi.org/10.1016/j.ijpsycho.2008.12.017.

Baizer, J. S., Ungerleider, L. G., & Desimone, R. (1991). Organization of visual inputs to the inferior temporal and posterior parietal cortex in macaques. *The Journal of Neuroscience: The Official Journal of the Society for Neuroscience, 11*(1), 168–190.

Bartolomeo, P., Bourgeois, A., Bourlon, C., & Migliaccio, R. (2013). Visual and motor mental imagery after brain damage. In *Multisensory imagery* (pp. 249–269). New York, NY: Springer. Retrieved from https://link.springer.com/chapter/10.1007/978-1-4614-5879-1_13.

Battistoni, E., Stein, T., & Peelen, M. V. (2017). Preparatory attention in visual cortex. *Annals of the New York Academy of Sciences, 1396*(1), 92–107. https://doi.org/10.1111/nyas.13320.

Behrens, T. E. J., Fox, P., Laird, A., & Smith, S. M. (2013). What is the most interesting part of the brain? *Trends in Cognitive Sciences, 17*(1), 2–4. https://doi.org/10.1016/j.tics.2012.10.010.

Belardinelli, M., Palmiero, M., Sestieri, C., Nardo, D., Di Matteo, R., Londei, A., et al. (2009). An fMRI investigation on image generation in different sensory modalities: The influence of vividness. *Acta Psychologica, 132*(2). https://doi.org/10.1016/j.actpsy.2009.06.009.

Bien, N., & Sack, A. T. (2014). Dissecting hemisphere-specific contributions to visual spatial imagery using parametric brain mapping. *NeuroImage, 94*, 231–238. https://doi.org/10.1016/j.neuroimage.2014.03.006.

Binder, J. R., Desai, R. H., Graves, W. W., & Conant, L. L. (2009). Where is the semantic system? A critical review and meta-analysis of 120 functional neuroimaging studies. *Cerebral Cortex, 19*(12), 2767–2796. https://doi.org/10.1093/cercor/bhp055.

Block, N. (1983). Mental pictures and cognitive science. *Philosophical Review, 92*(4), 499–542.

Boccia, M., Piccardi, L., Palermo, L., Nemmi, F., Sulpizio, V., Galati, G., et al. (2015). A penny for your thoughts! Patterns of fMRI activity reveal the content and the spatial topography of visual mental images. *Human Brain Mapping, 36*(3), 945–958. https://doi.org/10.1002/hbm.22678.

Bohland, J. W., Bokil, H., Allen, C. B., & Mitra, P. P. (2009). The brain atlas concordance problem: Quantitative comparison of anatomical parcellations. *PLoS One, 4*(9), e7200. https://doi.org/10.1371/journal.pone.0007200.

de Borst, A. W., Sack, A. T., Jansma, B. M., Esposito, F., de Martino, F., Valente, G., et al. (2012). Integration of "what" and "where" in frontal cortex during visual imagery of scenes. *NeuroImage, 60*(1), 47–58. https://doi.org/10.1016/j.neuroimage.2011.12.005.

Bowden, D. M., & Dubach, M. F. (2003). NeuroNames 2002. *Neuroinformatics, 1*(1), 43–59. https://doi.org/10.1385/NI:1:1:043.

Bressler, S. L., Tang, W., Sylvester, C. M., Shulman, G. L., & Corbetta, M. (2008). Top-down control of human visual cortex by frontal and parietal cortex in anticipatory visual spatial attention. *Journal of Neuroscience, 28*(40), 10056–10061. https://doi.org/10.1523/JNEUROSCI.1776-08.2008.

Brett, M., Johnsrude, I. S., & Owen, A. M. (2002). The problem of functional localization in the human brain. *Nature Reviews. Neuroscience, 3*(3), 243–249. https://doi.org/10.1038/nrn756.

Bruce, C. J., Goldberg, M. E., Bushnell, M. C., & Stanton, G. B. (1985). Primate frontal eye fields. II. Physiological and anatomical correlates of electrically evoked eye movements. *Journal of Neurophysiology, 54*(3), 714–734.

Button, K. S., Ioannidis, J. P. A., Mokrysz, C., Nosek, B. A., Flint, J., Robinson, E. S. J., et al. (2013). Power failure: Why small sample size undermines the reliability of neuroscience. *Nature Reviews Neuroscience, 14*(5), 365–376. https://doi.org/10.1038/nrn3475.

Buxton, R. B. (2002). *Introduction to functional magnetic resonance imaging: Principles and techniques*. Cambridge University Press. Retrieved from http://books.google.co.uk/books?id=pi3ogRUXxgYC.

Carp, J. (2012). The secret lives of experiments: Methods reporting in the fMRI literature. *NeuroImage, 63*(1), 289–300. https://doi.org/10.1016/j.neuroimage.2012.07.004.

Caspers, S., Amunts, K., & Zilles, K. (2012). Posterior parietal cortex: Multimodal association cortex. In J. Mai, & G. Paxinos (Eds.), *The human nervous system* (3rd ed., pp. 1036–1055). San Diego: Academic Press. Retrieved from http://www.sciencedirect.com/science/article/pii/B9780123742360100288.

Charlot, V., Tzourio, N., Zilbovicius, M., Mazoyer, B., & Denis, M. (1992). Different mental imagery abilities result in different regional cerebral blood flow activation patterns during cognitive tasks. *Neuropsychologia, 30*(6), 565–580. https://doi.org/10.1016/0028-3932(92)90059-U.

Choi, H.-J., Zilles, K., Mohlberg, H., Schleicher, A., Fink, G. R., Armstrong, E., et al. (2006). Cytoarchitectonic identification and probabilistic mapping of two distinct areas within the anterior ventral bank of the human intraparietal sulcus. *The Journal of Comparative Neurology, 495*(1), 53–69. https://doi.org/10.1002/cne.20849.

Chouinard, P. A., Morrissey, B. F., Köhler, S., & Goodale, M. A. (2008). Repetition suppression in occipital-temporal visual areas is modulated by physical rather than semantic features of objects. *NeuroImage, 41*(1), 130–144. https://doi.org/10.1016/j.neuroimage.2008.02.011.

Cichy, R. M., Heinzle, J., & Haynes, J.-D. (2012). Imagery and perception share cortical representations of content and location. *Cerebral Cortex, 22*(2), 372–380. https://doi.org/10.1093/cercor/bhr106.

Corbetta, M., & Shulman, G. L. (2002). Control of goal-directed and stimulus-driven attention in the brain. *Nature Reviews Neuroscience, 3*(3), 201–215. https://doi.org/10.1038/nrn755.

Cui, X., Jeter, C. B., Yang, D., Montague, P. R., & Eagleman, D. M. (2007). Vividness of mental imagery: Individual variability can be measured objectively. *Vision Research, 47*(4), 474–478. https://doi.org/10.1016/j.visres.2006.11.013.

David, S. P., Ware, J. J., Chu, I. M., Loftus, P. D., Fusar-Poli, P., Radua, J., et al. (2013). Potential reporting bias in fMRI studies of the brain. *PLoS One, 8*(7), e70104. https://doi.org/10.1371/journal.pone.0070104.

Demb, J., Desmond, J., Wagner, A., Vaidya, C., Glover, G., & Gabrieli, J. (1995). Semantic encoding and retrieval in the left inferior prefrontal cortex - a functional MRI study of task-difficulty and process specificity. *Journal of Neuroscience, 15*(9), 5870–5878.

Dennet, D. (1978). *Brainstorms: Philosophical essays on mind and psychology: Brainstorms – philosophical essays on mind & psychology*. Cambridge, Mass: MIT Press.

Devlin, J. T., & Poldrack, R. A. (2007). In praise of tedious anatomy. *NeuroImage, 37*(4), 1033–1041. https://doi.org/10.1016/j.neuroimage.2006.09.055. discussion 1050-1058.

Dijkstra, N., Bosch, S., & van Gerven, M. A. J. (2017). Vividness of visual imagery depends on the neural overlap with perception in visual areas. *Journal of Neuroscience*. https://doi.org/10.1523/JNEUROSCI.3022-16.2016, 3022–16.

D'Esposito, M., Detre, J. A., Aguirre, G. K., Stallcup, M., Alsop, D. C., Tippet, L. J., et al. (1997). A functional MRI study of mental image generation. *Neuropsychologia, 35*(5), 725–730.

Eickhoff, S. B., Bzdok, D., Laird, A. R., Kurth, F., & Fox, P. T. (2012). Activation likelihood estimation meta-analysis revisited. *NeuroImage, 59*(3), 2349–2361. https://doi.org/10.1016/j.neuroimage.2011.09.017.

Eickhoff, S. B., Laird, A. R., Grefkes, C., Wang, L. E., Zilles, K., & Fox, P. T. (2009). Coordinate-based ALE meta-analysis of neuroimaging data: A random-effects approach based on empirical estimates of spatial uncertainty. *Human Brain Mapping, 30*(9), 2907–2926. https://doi.org/10.1002/hbm.20718.

Eickhoff, S. B., Nichols, T. E., Laird, A. R., Hoffstaedter, F., Amunts, K., Fox, P. T., et al. (2016). Behavior, sensitivity, and power of activation likelihood estimation characterized by massive empirical simulation. *NeuroImage, 137*, 70–85. https://doi.org/10.1016/j.neuroimage.2016.04.072.

Evans, A. C., Janke, A. L., Collins, D. L., & Baillet, S. (2012). Brain templates and atlases. *NeuroImage, 62*(2), 911–922. https://doi.org/10.1016/j.neuroimage.2012.01.024.

Farah, M. (1994). *Beyond 'pet' methodologies to converging evidence*. Retrieved from http://www.sciencedirect.com/science/article/pii/016622369490152X.

Federative Committee on Anatomical Terminology. (1998). *Terminologia anatomica: International anatomical terminology* (1st ed.). Stuttgart: Thieme Stuttgart.

Finke, R. A. (1989). *Principles of mental imagery*. MIT Press.

Fischl, B., Rajendran, N., Busa, E., Augustinack, J., Hinds, O., Yeo, B. T. T., et al. (2008). Cortical folding patterns and predicting cytoarchitecture. *Cerebral Cortex (New York, N.Y.:*

1991), 18(8), 1973–1980. https://doi.org/10.1093/cercor/bhm225.
Fodor, J. A. (1975). *The language of thought*. Cambridge, Mass: Harvard University Press.
Formisano, E., Linden, D. E. J., Di Salle, F., Trojano, L., Esposito, F., Sack, A. T., et al. (2002). Tracking the mind's image in the brain I: Time-resolved fMRI during visuospatial mental imagery. *Neuron, 35*(1), 185–194.
Fox, P. T., Lancaster, J. L., Laird, A. R., & Eickhoff, S. B. (2014). Meta-analysis in human neuroimaging: Computational modeling of large-scale databases. *Annual Review of Neuroscience, 37*, 409–434. https://doi.org/10.1146/annurev-neuro-062012-170320.
Ganis, G., Thompson, W. L., & Kosslyn, S. M. (2004). Brain areas underlying visual mental imagery and visual perception: An fMRI study. *Brain Research. Cognitive Brain Research, 20*(2), 226–241. https://doi.org/10.1016/j.cogbrainres.2004.02.012.
Gardini, S., Cornoldi, C., De Beni, R., & Venneri, A. (2009). Cognitive and neuronal processes involved in sequential generation of general and specific mental images. *Psychological Research, 73*(5), 633–643. https://doi.org/10.1007/s00426-008-0175-1.
Gazzaley, A., & Nobre, A. C. (2012). Top-down modulation: Bridging selective attention and working memory. *Trends in Cognitive Sciences, 16*(2), 129–135. https://doi.org/10.1016/j.tics.2011.11.014.
Geyer, S., Luppino, G., & Rozzi, S. (2012). Motor cortex. In J. K. Mai, & G. Paxinos (Eds.), *The human nervous system* (3rd ed., pp. 1012–1035). San Diego: Academic Press. Retrieved from http://www.sciencedirect.com/science/article/pii/B9780123742360100276.
Gilmore, R. O., Diaz, M. T., Wyble, B. A., & Yarkoni, T. (2017). Progress toward openness, transparency, and reproducibility in cognitive neuroscience. *Annals of the New York Academy of Sciences, 1396*(1), 5–18. https://doi.org/10.1111/nyas.13325.
Glasser, M. F., Coalson, T. S., Robinson, E. C., Hacker, C. D., Harwell, J., Yacoub, E., et al. (2016). A multi-modal parcellation of human cerebral cortex. *Nature, 536*(7615), 171–178. https://doi.org/10.1038/nature18933.
Glasser, M. F., & Van Essen, D. C. (2011). Mapping human cortical areas in vivo based on myelin content as revealed by T1- and T2-weighted MRI. *The Journal of Neuroscience: The Official Journal of the Society for Neuroscience, 31*(32), 11597–11616. https://doi.org/10.1523/JNEUROSCI.2180-11.2011.
Glatard, T., Lewis, L. B., Ferreira da Silva, R., Adalat, R., Beck, N., Lepage, C., et al. (2015). Reproducibility of neuroimaging analyses across operating systems. *Frontiers in Neuroinformatics, 9*. https://doi.org/10.3389/fninf.2015.00012.
Goldenberg, G., Podreka, I., Steiner, M., Willmes, K., Suess, E., & Deecke, L. (1989). Regional cerebral blood flow patterns in visual imagery. *Neuropsychologia, 27*(5), 641–664. https://doi.org/10.1016/0028-3932(89)90110-3.
Greenberg, A. S., Esterman, M., Wilson, D., Serences, J. T., & Yantis, S. (2010). Control of spatial and feature-based attention in frontoparietal cortex. *Journal of Neuroscience, 30*(43), 14330–14339. https://doi.org/10.1523/JNEUROSCI.4248-09.2010.
Grill-Spector, K., & Weiner, K. S. (2014). The functional architecture of the ventral temporal cortex and its role in categorization. *Nature Reviews Neuroscience, 15*(8), 536–548. https://doi.org/10.1038/nrn3747.
Gulyas, B. (2001). Neural networks for internal reading and visual imagery of reading: A PET study. *Brain Research Bulletin, 54*(3), 319–328.
Hagler, D. J., Riecke, L., & Sereno, M. I. (2007). Parietal and superior frontal visuospatial maps activated by pointing and saccades. *NeuroImage, 35*(4), 1562–1577. https://doi.org/10.1016/j.neuroimage.2007.01.033.
Handy, T. C., Miller, M. B., Schott, B., Shroff, N. M., Janata, P., Van Horn, J. D., et al. (2004). Visual imagery and memory: Do retrieval strategies affect what the mind's eye sees? *European Journal of Cognitive Psychology, 16*(5), 631–652. https://doi.org/10.1080/09541440340000457.
Hetu, S., Gregoire, M., Saimpont, A., Coll, M.-P., Eugene, F., Michon, P.-E., et al. (2013). The neural network of motor imagery: An ALE meta-analysis. *Neuroscience and Biobehavioral Reviews, 37*(5), 930–949. https://doi.org/10.1016/j.neubiorev.2013.03.017.
Holmes, E. A., & Mathews, A. (2010). Mental imagery in emotion and emotional disorders. *Clinical Psychology Review, 30*(3), 349–362. https://doi.org/10.1016/j.cpr.2010.01.001.
Hume, D. (1784). *An enquiry concerning human understanding*. Simon & Brown.
Ishai, A. (2010). Seeing with the mind's eye: Top-down, bottom-up, and conscious awareness. *F1000 Biology Reports, 2*. https://doi.org/10.3410/b2-34.
Ishai, A., Ungerleider, L., & Haxby, J. (2000). Distributed neural systems for the generation of visual images. *Neuron, 28*(3), 979–990.
Jenkinson, M., Bannister, P., Brady, M., & Smith, S. (2002). Improved optimization for the robust and accurate linear registration and motion correction of brain images. *NeuroImage, 17*(2), 825–841. https://doi.org/10.1006/nimg.2002.1132.
Kamitani, Y., & Tong, F. (2005). Decoding the visual and subjective contents of the human brain. *Nature Neuroscience, 8*(5), 679–685. https://doi.org/10.1038/nn1444.
Keogh, R., & Pearson, J. (2014). The sensory strength of voluntary visual imagery predicts visual working memory capacity. *Journal of Vision, 14*(12). https://doi.org/10.1167/14.12.7.
Klein, I., Paradis, A.-L., Poline, J.-B., Kosslyn, S. M., & Le Bihan, D. (2000). Transient activity in the human calcarine cortex during visual-mental Imagery: An event-related fMRI study. *Journal of Cognitive Neuroscience, 12*(Suppl. 2), 15–23. https://doi.org/10.1162/089892900564037.
Knauff, M., Kassubek, J., Mulack, T., & Greenlee, M. W. (2000). Cortical activation evoked by visual mental imagery as measured by fMRI. *NeuroReport, 11*(18), 3957–3962.
Kosslyn, S. (1981). The medium and the message in mental imagery: A theory. In N. Block (Ed.), *Imagery*. MIT Press.
Kosslyn, S. (2005). Mental images and the brain. *Cognitive Neuropsychology, 22*(3), 333–347. https://doi.org/10.1080/02643290442000130.
Kosslyn, S., Alpert, N., Thompson, W., Maljkovic, V., Weise, S., Chabris, C., et al. (1993). Visual mental imagery activates topographically organized visual cortex: PET investigations. *Journal of Cognitive Neuroscience, 5*(3), 263–287. https://doi.org/10.1162/jocn.1993.5.3.263.
Kosslyn, S., & Ochsner, K. N. (1994). In search of occipital activation during visual mental imagery. *Trends in Neurosciences, 17*(7), 290–292. https://doi.org/10.1016/0166-2236(94)90059-0.
Kosslyn, S., & Thompson, W. (2003). When is early visual cortex activated during visual mental imagery? *Psychological Bulletin, 129*(5), 723–746. https://doi.org/10.1037/0033-2909.129.5.723.
Kosslyn, S., Thompson, W., & Alpert, N. (1997). Neural systems shared by visual imagery and visual perception: A positron emission tomography study. *NeuroImage, 6*(4), 320–334. https://doi.org/10.1006/nimg.1997.0295.
Kosslyn, S., Thompson, W., Kim, I., & Alpert, N. (1995). Topographical representations of mental images in primary visual cortex. *Nature, 378*(6556), 496–498. https://doi.org/10.1038/378496a0.
Kosslyn, S., Thompson, W., Sukel, K., & Alpert, N. (2005). Two types of image generation: Evidence from PET. *Cognitive, Affective & Behavioral Neuroscience, 5*(1).

Kukolja, J., Marshall, J. C., & Fink, G. R. (2006). Neural mechanisms underlying spatial judgements on seen and imagined visual stimuli in the left and right hemifields in men. *Neuropsychologia, 44*(14), 2846–2860. https://doi.org/10.1016/j.neuropsychologia.2006.06.029.

Laird, A. R., Fox, P. M., Price, C. J., Glahn, D. C., Uecker, A. M., Lancaster, J. L., et al. (2005). ALE meta-analysis: Controlling the false discovery rate and performing statistical contrasts. *Human Brain Mapping, 25*(1), 155–164. https://doi.org/10.1002/hbm.20136.

Laird, A. R., Robinson, J. L., McMillan, K. M., Tordesillas-Gutiérrez, D., Moran, S. T., Gonzales, S. M., et al. (2010). Comparison of the disparity between Talairach and MNI coordinates in functional neuroimaging data: Validation of the lancaster transform. *NeuroImage, 51*(2), 677–683. https://doi.org/10.1016/j.neuroimage.2010.02.048.

Lambert, S., Sampaio, E., Scheiber, C., & Mauss, Y. (2002). Neural substrates of animal mental imagery: Calcarine sulcus and dorsal pathway involvement–an fMRI study. *Brain Research, 924*(2), 176–183.

Lancaster, J. L., Tordesillas-Gutiérrez, D., Martinez, M., Salinas, F., Evans, A., Zilles, K., et al. (2007). Bias between MNI and Talairach coordinates analyzed using the ICBM-152 brain template. *Human Brain Mapping, 28*(11), 1194–1205. https://doi.org/10.1002/hbm.20345.

Lancaster, J. L., Woldorff, M. G., Parsons, L. M., Liotti, M., Freitas, C. S., Rainey, L., et al. (2000). Automated Talairach atlas labels for functional brain mapping. *Human Brain Mapping, 10*(3), 120–131.

Lauritzen, T. Z., D'Esposito, M., Heeger, D. J., & Silver, M. A. (2009). Top–down flow of visual spatial attention signals from parietal to occipital cortex. *Journal of Vision, 9*(13). https://doi.org/10.1167/9.13.18, 18.1-1814.

Le Bihan, D., Turner, R., Zeffiro, T. A., Cuénod, C. A., Jezzard, P., & Bonnerot, V. (1993). Activation of human primary visual cortex during visual recall: A magnetic resonance imaging study. *Proceedings of the National Academy of Sciences of the United States of America, 90*(24), 11802–11805.

Leber, A. B. (2010). Neural predictors of within-subject fluctuations in attentional control. *The Journal of Neuroscience: The Official Journal of the Society for Neuroscience, 30*(34), 11458–11465. https://doi.org/10.1523/JNEUROSCI.0809-10.2010.

Lee, S.-H., Kravitz, D. J., & Baker, C. I. (2012). Disentangling visual imagery and perception of real-world objects. *NeuroImage, 59*(4), 4064–4073. https://doi.org/10.1016/j.neuroimage.2011.10.055.

Lewis, J. W., & Van Essen, D. C. (2000). Corticocortical connections of visual, sensorimotor, and multimodal processing areas in the parietal lobe of the macaque monkey. *The Journal of Comparative Neurology, 428*(1), 112–137.

Liu, J., Li, J., Feng, L., Li, L., Tian, J., & Lee, K. (2014). Seeing Jesus in toast: Neural and behavioral correlates of face pareidolia. *Cortex, 53*, 60–77. https://doi.org/10.1016/j.cortex.2014.01.013.

Mackey, W. E., Winawer, J., & Curtis, C. E. (2017). Visual field map clusters in human frontoparietal cortex. *Elife, 6*, e22974. https://doi.org/10.7554/eLife.22974.

MacKisack, M., Aldworth, S., Macpherson, F., Onians, J., Winlove, C., & Zeman, A. (2016). On picturing a candle: The prehistory of imagery science. *Perception Science, 515*. https://doi.org/10.3389/fpsyg.2016.00515.

Mai, J., & Paxinos, G. (Eds.). (2012). *The human nervous system*. San Diego: Academic Press. Retrieved from http://www.sciencedirect.com/science/article/pii/B9780123742360100410.

Markov, N. T., Vezoli, J., Chameau, P., Falchier, A., Quilodran, R., Huissoud, C., et al. (2014). Anatomy of hierarchy: Feedforward and feedback pathways in macaque visual cortex. *The Journal of Comparative Neurology, 522*(1), 225–259. https://doi.org/10.1002/cne.23458.

Mazard, A., Laou, L., Joliot, M., & Mellet, E. (2005). Neural impact of the semantic content of visual mental images and visual percepts. *Brain Research. Cognitive Brain Research, 24*(3), 423–435. https://doi.org/10.1016/j.cogbrainres.2005.02.018.

McMahon, C. E. (1973). Images as motives and motivators: A historical perspective. *The American Journal of Psychology, 86*(3), 465–490. https://doi.org/10.2307/1421935.

Mechelli, A., Price, C., Friston, K., & Ishai, A. (2004). Where bottom-up meets top-down: Neuronal interactions during perception and imagery. *Cerebral Cortex (New York, N.Y.: 1991), 14*(11), 1256–1265. https://doi.org/10.1093/cercor/bhh087.

Mellet, E., Tzourio-Mazoyer, N., Bricogne, S., Mazoyer, B., Kosslyn, S. M., & Denis, M. (2000). Functional anatomy of high-resolution visual mental imagery. *Journal of Cognitive Neuroscience, 12*(1).

Mellet, E., Tzourio, N., Crivello, F., Joliot, M., Denis, M., & Mazoyer, B. (1996). Functional anatomy of spatial mental imagery generated from verbal instructions. *The Journal of Neuroscience: The Official Journal of the Society for Neuroscience, 16*(20), 6504–6512.

Mellet, E., Tzourio, N., Denis, M., & Mazoyer, B. (1995). A positron emission tomography study of visual and mental spatial exploration. *Journal of Cognitive Neuroscience, 7*(4), 433–445. https://doi.org/10.1162/jocn.1995.7.4.433.

Mellet, E., Tzourio, N., Denis, M., & Mazoyer, B. (1998). Cortical anatomy of mental imagery of concrete nouns based on their dictionary definition. *NeuroReport, 9*(5), 803–808.

Mithen, S. (1998). *The prehistory of the mind: A search for the origins of art, religion and science*. London: Weidenfeld & Nicolson.

Modrak. (1987). *Aristotle: The power of perception*. Chicago: University of Chicago Press.

Moore, T., & Armstrong, K. M. (2003). Selective gating of visual signals by microstimulation of frontal cortex. *Nature, 421*(6921), 370–373. https://doi.org/10.1038/nature01341.

Moreira, P. S., Marques, P., & Magalhães, R. (2016). Identifying functional subdivisions in the medial frontal cortex. *Journal of Neuroscience, 36*(44), 11168–11170. https://doi.org/10.1523/JNEUROSCI.2584-16.2016.

Muckli, L., & Petro, L. S. (2013). Network interactions: Non-geniculate input to V1. *Current Opinion in Neurobiology, 23*(2), 195–201. https://doi.org/10.1016/j.conb.2013.01.020.

Naselaris, T., Olman, C. A., Stansbury, D. E., Ugurbil, K., & Gallant, J. L. (2015). A voxel-wise encoding model for early visual areas decodes mental images of remembered scenes. *NeuroImage, 105*, 215–228. https://doi.org/10.1016/j.neuroimage.2014.10.018.

Neisser, U. (1967). *Cognitive psychology*. New York: Appleton-Century-Crofts.

Nieuwenhuys, R., Broere, C. A. J., & Cerliani, L. (2015). A new myeloarchitectonic map of the human neocortex based on data from the Vogt-Vogt school. *Brain Structure & Function, 220*(5), 2551–2573. https://doi.org/10.1007/s00429-014-0806-9.

Okano, H., & Yamamori, T. (2016). How can brain mapping initiatives cooperate to achieve the same goal? *Nature Reviews Neuroscience, 17*(12), 733–734. https://doi.org/10.1038/nrn.2016.126.

Paivio, A. (1978). Comparisons of mental clocks. *Journal of Experimental Psychology. Human Perception and Performance, 4*(1), 61–71.

Palmer, T. M., & Sterne, J. A. C. (2015). *Meta-analysis in Stata: An updated collection from the Stata Journal* (2nd ed.). Texas: Stata Press.

Pearson, J., Naselaris, T., Holmes, E. A., & Kosslyn, S. M. (2015). Mental imagery: Functional mechanisms and clinical applications. *Trends in Cognitive Sciences, 19*(10), 590–602. https://doi.org/10.1016/j.tics.2015.08.003.

Peelen, M. V., & Kastner, S. (2011). A neural basis for real-world visual search in human occipitotemporal cortex. *Proceedings of*

the National Academy of Sciences, 108(29), 12125–12130. https://doi.org/10.1073/pnas.1101042108.
Petrides, M., & Pandya, D. N. (1999). Dorsolateral prefrontal cortex: Comparative cytoarchitectonic analysis in the human and the macaque brain and corticocortical connection patterns. *The European Journal of Neuroscience, 11*(3), 1011–1036.
Petrides, M., & Pandya, D. (2012). The frontal cortex. In J. Mai, & G. Paxinos (Eds.), *The human nervous system* (3rd ed., pp. 988–1011). San Diego: Academic Press. Retrieved from http://www.sciencedirect.com/science/article/pii/B9780123742360100264.
Poldrack, R. (2006). Can cognitive processes be inferred from neuroimaging data? *Trends in Cognitive Sciences, 10*(2), 59–63. https://doi.org/10.1016/j.tics.2005.12.004.
Poldrack, R. (2011). Inferring mental states from neuroimaging data: From reverse inference to large-scale decoding. *Neuron, 72*(5), 692–697. https://doi.org/10.1016/j.neuron.2011.11.001.
Poldrack, R., Wagner, A., Prull, M., Desmond, J., Glover, G., & Gabrieli, J. (1999). Functional specialization for semantic and phonological processing in the left inferior prefrontal cortex. *NeuroImage, 10*(1), 15–35. https://doi.org/10.1006/nimg.1999.0441.
Pylyshyn, Z. (2003). Return of the mental image: Are there really pictures in the brain? *Trends in Cognitive Sciences, 7*(3), 113–118. https://doi.org/10.1016/S1364-6613(03)00003-2.
Richardson, J. T. E. (1998). *Imagery* (1st ed.). Hove, East Sussex, UK: Routledge.
Roland, P. E., & Friberg, L. (1985). Localization of cortical areas activated by thinking. *Journal of Neurophysiology, 53*(5), 1219–1243.
Roland, P. E., & Gulyás, B. (1994a). Visual imagery and visual representation. *Trends in Neurosciences, 17*(7), 281–287. https://doi.org/10.1016/0166-2236(94)90057-4.
Roland, P. E., & Gulyás, B. (1994b). Visual representations of scenes and objects: Retinotopical or non-retinotopical? *Trends in Neurosciences, 17*(7), 294–297. https://doi.org/10.1016/0166-2236(94)90061-2.
Roland, P. E., & Zilles, K. (1996). Functions and structures of the motor cortices in humans. *Current Opinion in Neurobiology, 6*(6), 773–781.
Rosse, C., & Mejino, J. L. V. (2003). A reference ontology for biomedical informatics: The foundational model of anatomy. *Journal of Biomedical Informatics, 36*(6), 478–500. https://doi.org/10.1016/j.jbi.2003.11.007.
Rubin, D. L., Lewis, S. E., Mungall, C. J., Misra, S., Westerfield, M., Ashburner, M., et al. (2006). National center for biomedical ontology: Advancing biomedicine through structured organization of scientific knowledge. *Omics: A Journal of Integrative Biology, 10*(2), 185–198. https://doi.org/10.1089/omi.2006.10.185.
Ruff, C. C., Blankenburg, F., Bjoertomt, O., Bestmann, S., Freeman, E., Haynes, J.-D., et al. (2006). Concurrent TMS-fMRI and psychophysics reveal frontal influences on human retinotopic visual cortex. *Current Biology, 16*(15), 1479–1488. https://doi.org/10.1016/j.cub.2006.06.057.
Russell, B. (1921). *The analysis of mind*. CreateSpace Independent Publishing Platform.
Sack, A. T., Camprodon, J. A., Pascual-Leone, A., & Goebel, R. (2005). The dynamics of interhemispheric compensatory processes in mental imagery. *Science (New York, N.Y.), 308*(5722), 702–704. https://doi.org/10.1126/science.1107784.
Sack, A. T., Sperling, J. M., Prvulovic, D., Formisano, E., Goebel, R., Di Salle, F., et al. (2002). Tracking the mind's image in the brain II: Transcranial magnetic stimulation reveals parietal asymmetry in visuospatial imagery. *Neuron, 35*(1).
Serences, J. T. (2008). Value-based modulations in human visual cortex. *Neuron, 60*(6), 1169–1181. https://doi.org/10.1016/j.neuron.2008.10.051.
Shulman, G. L., Fiez, J. A., Corbetta, M., Buckner, R. L., Miezin, F. M., Raichle, M. E., et al. (1997). Common blood flow changes across visual tasks. 2. Decreases in cerebral cortex. *Journal of Cognitive Neuroscience, 9*(5), 648–663. https://doi.org/10.1162/jocn.1997.9.5.648.
Smith, M. L., Gosselin, F., & Schyns, P. G. (2012). Measuring internal representations from behavioral and brain data. *Current Biology, 22*(3), 191–196. https://doi.org/10.1016/j.cub.2011.11.061.
Stark, C. E. L., & Squire, L. R. (2001). When zero is not zero: The problem of ambiguous baseline conditions in fMRI. *Proceedings of the National Academy of Sciences, 98*(22), 12760–12766. https://doi.org/10.1073/pnas.221462998.
Talairach, J., & Tournoux, P. (1988). *Co-planar stereotaxic atlas of the human brain: 3-Dimensional proportional system - An approach to cerebral imaging*. New York: Thieme Medical Publishers.
Thomas, N. (2003). Imagining minds. *Journal of Consciousness Studies, 10*(11), 79–84.
Thomas, N. (2014a). Mental imagery. In *Stanford encyclopedia of philosophy*. Retrieved from https://leibniz.stanford.edu/friends/members/preview/mental-imagery/.
Thomas, N. (2014b). The multidimensional spectrum of Imagination: Images, dreams, hallucinations, and active, imaginative perception. *Humanities, 3*(2), 132–184.
Thompson-Schill, S. L., Aguirre, G. K., D'Esposito, M., & Farah, M. J. (1999). A neural basis for category and modality specificity of semantic knowledge. *Neuropsychologia, 37*(6), 671–676.
Thompson-Schill, S. L., D'Esposito, M., Aguirre, G. K., & Farah, M. J. (1997). Role of left inferior prefrontal cortex in retrieval of semantic knowledge: A reevaluation. *Proceedings of the National Academy of Sciences of the United States of America, 94*(26), 14792–14797. https://doi.org/10.1073/pnas.94.26.14792.
Toga, A. W., & Thompson, P. M. (2007). What is where and Why it is Important. *NeuroImage, 37*(4), 1045–1068. https://doi.org/10.1016/j.neuroimage.2007.02.018.
Triarhou, L. C. (2007). A proposed number system for the 107 cortical areas of Economo and Koskinas, and Brodmann area correlations. *Stereotactic and Functional Neurosurgery, 85*(5), 204–215. https://doi.org/10.1159/000103259.
Trojano, L., Grossi, D., Linden, D. E., Formisano, E., Hacker, H., Zanella, F. E., et al. (2000). Matching two imagined clocks: The functional anatomy of spatial analysis in the absence of visual stimulation. *Cerebral Cortex (New York, N.Y.: 1991), 10*(5), 473–481.
Turkeltaub, P., Eden, G. F., Jones, K. M., & Zeffiro, T. A. (2002). Meta-analysis of the functional neuroanatomy of single-word reading: Method and validation. *NeuroImage, 16*(3), 765–780. https://doi.org/10.1006/nimg.2002.1131.
Turkeltaub, P., Eickhoff, S. B., Laird, A. R., Fox, M., Wiener, M., & Fox, P. (2012). Minimizing within-experiment and within-group effects in activation likelihood estimation meta-analyses. *Human Brain Mapping, 33*(1), 1–13. https://doi.org/10.1002/hbm.21186.
Tye, M. (1991). *The imagery debate*. MIT Press. Retrieved from http://books.google.com/books?hl=en&lr=&id=r_hV7ZjmCe8C&oi=fnd&pg=PR9&dq=%22The+Physical+Realization+of+Imagery+in+the+Brain%22+%22Imagistic+Representation:+My+Own%22+%22What+It+Is+That+Shoemaker+Likes%22+%22The+Causal+Role+of+Image+Content%22+%22What+Are+Visual%22+&ots=jqSkZx1OCr&sig=pe6UVFrjAHHKV0-vYFWJtax3r1M.
Van Essen, D. C., Glasser, M. F., Dierker, D. L., & Harwell, J. (2012). Cortical parcellations of the macaque monkey analyzed on surface-based atlases. *Cerebral Cortex (New York, N.Y.: 1991), 22*(10), 2227–2240. https://doi.org/10.1093/cercor/bhr290.
Van Ettinger-Veenstra, H. M., Huijbers, W., Gutteling, T. P., Vink, M., Kenemans, J. L., & Neggers, S. F. W. (2009). fMRI-

guided TMS on cortical eye fields: the frontal but not intraparietal eye fields regulate the coupling between visuospatial attention and eye movements. *Journal of Neurophysiology, 102*(6), 3469–3480. https://doi.org/10.1152/jn.00350.2009.

Vandenberghe, R., Price, C., Wise, R., Josephs, O., & Frackowiak, R. S. J. (1996). Functional anatomy of a common semantic system for words and pictures. *Nature, 383*(6597), 254–256. https://doi.org/10.1038/383254a0.

Vetter, P., Smith, F. W., & Muckli, L. (2014). Decoding sound and imagery content in early visual cortex. *Current Biology, 24*(11), 1256–1262. https://doi.org/10.1016/j.cub.2014.04.020.

Vogt, B., & Palomero-Gallagher, N. (2012). Cingulate cortex. In J. A. J. Schmitt, & G. Paxinos (Eds.), *The human nervous system* (3rd ed., pp. 943–987). San Diego: Academic Press. Retrieved from http://www.sciencedirect.com/science/article/pii/B9780123742360100252.

Vossel, S., Geng, J. J., & Fink, G. R. (2014). Dorsal and ventral attention systems: Distinct neural circuits but collaborative roles. *The Neuroscientist: A Review Journal Bringing Neurobiology, Neurology and Psychiatry, 20*(2), 150–159. https://doi.org/10.1177/1073858413494269.

Wager, T. D., & Smith, E. E. (2003). Neuroimaging studies of working memory: A meta-analysis. *Cognitive Affective & Behavioral Neuroscience, 3*(4), 255–274. https://doi.org/10.3758/CABN.3.4.255.

Waskom, M. L., & Wagner, A. D. (2017). Distributed representation of context by intrinsic subnetworks in prefrontal cortex. *Proceedings of the National Academy of Sciences of the United States of America, 114*(8), 2030–2035. https://doi.org/10.1073/pnas.1615269114.

Watson, J. B. (1913). Image and affection in behavior. *The Journal of Philosophy, Psychology and Scientific Methods, 10*(16), 421–428. https://doi.org/10.2307/2012899.

Weiner, K. S., Golarai, G., Caspers, J., Chuapoco, M. R., Mohlberg, H., Zilles, K., et al. (2014). The mid-fusiform sulcus: A landmark identifying both cytoarchitectonic and functional divisions of human ventral temporal cortex. *NeuroImage, 84*, 453–465. https://doi.org/10.1016/j.neuroimage.2013.08.068.

Wilder, B. G. (1896). Neural terms, international and national. *Journal of Comparative Neurology, 6*(3), 216–352. https://doi.org/10.1002/cne.910060306.

Willard, R. D. (1977). Breast enlargement through visual imagery and hypnosis. *The American Journal of Clinical Hypnosis, 19*(4), 195–200. https://doi.org/10.1080/00029157.1977.10403875.

Wittgenstein, L. (1953). In P. M. S. Hacker, & J. Schulte (Eds.), *Philosophical investigations* (4th ed.). Chichester, West Sussex, U.K.; Malden, MA: Wiley-Blackwell.

Wojciulik, E., & Kanwisher, N. (1999). The generality of parietal involvement in visual attention. *Neuron, 23*(4), 747–764.

Yarkoni, T., Poldrack, R. A., Nichols, T. E., Van Essen, D. C., & Wager, T. D. (2011). Large-scale automated synthesis of human functional neuroimaging data. *Nature Methods, 8*(8), 665–670. https://doi.org/10.1038/nmeth.1635.

Yates, F. A. (2014). *The art of memory*. London: Bodley Head.

Yomogida, Y., Sugiura, M., Watanabe, J., Akitsuki, Y., Sassa, Y., Sato, T., et al. (2004). Mental visual synthesis is originated in the fronto-temporal network of the left hemisphere. *Cerebral Cortex (New York, N.Y.: 1991), 14*(12), 1376–1383. https://doi.org/10.1093/cercor/bhh098.

Zvyagintsev, M., Clemens, B., Chechko, N., Mathiak, K. A., Sack, A. T., & Mathiak, K. (2013). Brain networks underlying mental imagery of auditory and visual information. *The European Journal of Neuroscience, 37*(9), 1421–1434. https://doi.org/10.1111/ejn.12140.